2013

Fabrication Of Metallic Antenna Arrays Using Nanoimprint Lithography

Yu-Wei Lin

University of Central Florida

FABRICATION OF METALLIC ANTENNA ARRAYS USING NANOIMPRINT LITHOGRAPHY

by

YU-WEI LIN
B.S. National Taiwan University of Science and Technology, 2010

A thesis submitted in partial fulfillment of the requirements
for the degree of Master of Science
in the College of Optics and Photonics
at the University of Central Florida
Orlando, Florida

Fall Term
2013

Major Professor: Pieter G. Kik

ABSTRACT

This Thesis describes the development of a cost-effective process for patterning nanoscale metal antenna arrays. Soft ultraviolet (UV) Nanoimprint Lithography (NIL) into bilayer resist was chosen since it enables repeatable large-scale replication of nanoscale patterns with good lift-off properties using a simple low-cost process.

Nanofabrication often involves the use of Electron Beam Lithography (EBL) which enables the definition of nanoscale patterns on small sample regions, typically < 1 mm^2. However its sequential nature makes the large scale production of nanostructured substrates using EBL cost-prohibitive. NIL is a pattern replication method that can reproduce nanoscale patterns in a parallel fashion, allowing the low-cost and rapid production of a large number of nano-patterned samples based on a single nanostructured master mold.

Standard NIL replicates patterns by pressing a nanostructured hard mold into a soft resist layer on a substrate resulting in exposed substrate regions, followed by an optional Reactive Ion Etching (RIE) step and the subsequent deposition of e.g. metal onto the exposed substrate area. However, non-vertical sidewalls of the features in the resist layer resulting from an imperfect hard mold, from reflow of the resist layer, or from isotropic etching in the RIE step

may cause imperfect lift-off. To overcome this problem, a bilayer resist method can be used. Using stacked resist layers with different etch rates, undercut structures can be obtained after the RIE step, allowing for easy lift-off even when using a mold with non-vertical sidewalls.

Experiments were carried out using a nanostructured negative SiO_2 master mold. Various material combinations and processing methods were explored. The negative master mold was transferred to a positive soft mold, leaving the original master mold unaltered. The soft mold consisted of a 5 μm thick top Poly(methyl methacrylate) (PMMA), or Polyvinyl alcohol (PVA) layer, a 1.5 mm thick Polydimethylsiloxane (PDMS) buffer layer, and a glass supporting substrate. The soft mold was pressed into a bilayer of 300 nm PMMA and 350 nm of silicon based UV-curable resist that was spin-coated onto a glass slide, and cured using UV radiation. The imprinted patterns were etched using RIE, exposing the substrate, followed by metal deposition and lift-off. The experiments show that the use of soft molds enables successful pattern transfer even in the presence of small dust particles between the mold and the resist layer. Feature sizes down to 280 nm were replicated successfully.

ACKNOWLEDGMENTS

I would like to express my greatest gratitude to my advisor Prof. Pieter G. Kik for his patience, motivation, and knowledge. He continually and persuasively guided me through my researches and writing for thesis. Without his supervision and help, I would not have had the chance to finish this thesis.

I would like to thank the rest of my thesis committees: Prof. Sasan Fathpour and Prof. Winston V. Schoenfeld, for their encouragements and supports.

In addition, my sincere appreciation goes to Prof. Hyoung Jin Cho for allowing me to use the nanoimprint machine, NX2500; and my group mates, Chatdanai Lumdee and Seyfollah Toroghi, for their numerous help in my life and research. Also, I appreciate Dr. Roxana Shabani and Edward Dein, who have helped me with using NX2500; Edris Sarailou and Dr. Abdullah Zakariya for their help with RIE and UV laser writing; students in Prof. Wu's group for assisting me weighting chemicals; Prof. Stephen Kuebler and his student, Chris Grabill, for helping me with storing TMCS; Prof. Robert Peale and his student, Deep Panjwani, for the help with metal deposition; Ryuichi Tsuchikawa for the help with SEM imaging; and all the students in CREOL who have helped me with my thesis research.

Last but not least, I would like to thank my family: my parents who continuously support my Master study, and my sisters' family who take care of me during my time in United States.

TABLE OF CONTENTS

LIST OF FIGURES

LIST OF TABLES

CHAPTER ONE: INTRODUCTION

Plasmonics is a technology that makes use of the interaction between electromagnetic waves and metallic structures at the nanometer scale. The oscillatory electric field of the electromagnetic wave drives free electrons in metallic nanostructures to oscillate. The oscillations of these electrons are collective and create an extraordinarily strong local field at a certain frequency, known as the plasmon resonance frequency. By changing the geometry of metallic structures, one can manipulate the optical properties of the materials; for example, controlling the absorption, reflection, and transmission spectrum of materials by using metal structures with different resonant frequencies[1]; creating highly-enhanced and confined electric fields around a metal nanostructure by matching its plasmon resonant frequency with incident light[2,3]. Plasmonics studies on metallic structures with different shapes, sizes, and materials have been widely conducted in the past decade[4,5,6,7,8]. Moreover, with the help of suitable nanofabrication techniques, the idea of plasmonics can be introduced to real applications, for example, waveguiding[9,10,11], biological applications: sensing[12,13], imaging and labeling[14,15], and, biophysics[16], device performance enhancement for: light sources[17], detectors[18], and photovoltaics[19,20]. In many of these applications, a large area pattern with numerous designed sub-wavelength plasmonic nanostructures is needed. In order to meet specific purposes, for example, for significant interaction of plasmonic structures with a

focused optical beam at least a ~10μm × 10μm area is needed for sensing experiments [21]; and $>10^4$ μm^2 area is needed for plasmonic structures cooperating with other devices that are usually hundreds of micron in size, such as light emitting diodes and solar cells. Therefore, the capability of producing large area samples containing high resolution nano-scale structures is becoming a crucial point in both industrial and academic plasmonics work. There are several conventional fabrication techniques that can pattern nanometer scale structures on desired surfaces such as Focused Ion Beam (FIB)[22] patterning and Electron Beam lithography (EBL)[23]. Figure 1 describes the fabrication procedure of EBL.

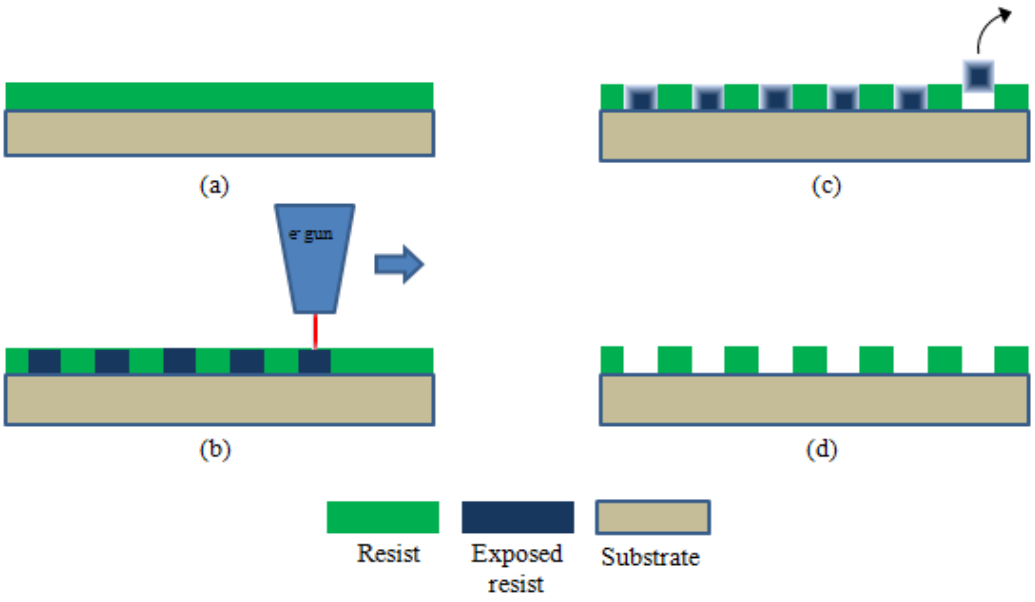

Figure 1. Schematic illustration of Electron Beam Lithography. (a) spin-coated resist layer (green) on substrate. (b) Electron beam direct writing resulting in exposed resist (blue). (c) developing exposed resist area. (d) Final patterned resist layer.

These two techniques, especially EBL, is commonly used for nanofabrication. However, when using EBL to pattern nanometer scale structures over a large area on a non-conductive

substrate, the sample often becomes highly charged which leads to deflection of the incoming writing beam resulting in distorting the sizes, shapes, and positions of designed patterns[24]. Besides, the time and cost needed for EBL to make samples with large area patterns are very long and prohibitive. Therefore, many alternative techniques have been developed in order to make the fabrication process faster and more cost-effective [4,25,26,27,28]. Among those alternative techniques, Nanoimprint lithography (NIL) possess the advantages of low cost, high throughput, high resolution, and large area fabrication. For these reasons NIL has the potential to become one of the most popular and cost-effective nanofabrication, or more precisely, nano-replication techniques.

Nanoimprint lithography relies on the replication of a single high-cost master structure. While the fabrication of the original master structure is expensive, the replication can be fast and low cost, making the technique viable for large scale production. It also allows for affordable parametric testing by making it feasible to try out multiple materials, multiple post-processing steps, and multiple destructive analyses all on low cost replicas of the original nanopattern. The general procedure of Nanoimprint lithography is as follows: first, fabricate a nanopattern on a hard substrate (master mold) by conventional nanofabrication techniques. Second, press the patterned the master mold into a resist layer on a hard substrate,

which allows the resist layer to be re-shaped to form a negative imprint of the master patterns. Third, separate mold from resist layer leaving the substrate with exposed area, where the resist has been squeezed out by the master mold during imprinting, as well as remaining resist-covered area. The remaining resist then serves as a mask in a subsequent metal deposition step carried out in vacuum. After metal deposition, metal that was deposited on the resist covered sections of the sample can be removed by dissolving and washing away the resist layer (Lift-off). After this step, a metal replica of the original designed positive patterns is obtained on the substrate. The nanoimprint process is a repeatable process based as long as the hard master mold is not damaged in the imprint process, which can be achieved with careful handling and cleaning of the hard maser mold. Thus, although the key element of Nanoimprint lithography, the hard imprint mold, needs to be patterned through costly nanofabrication techniques, the cost-per-sample can be low since the master mold is being reused. In addition, with proper methods, NIL can also be performed on non-planar surfaces in order to obtain three-dimension patterns.

This report mainly focuses on an approach where the imprint mold itself is a replica of a negative hard master mold. This avoids using the original hard master mold in any high-pressure imprint steps, further increasing the longevity of the hard master. To enable this,

relatively soft polymer materials will be used in the actual imprinting that will be hardened after imprint using ultraviolet (UV) exposure. This Soft UV-NIL process will be combined with a Bilayer imprint method to facilitate the lift-off process in the formation of large scale metallic antenna arrays. Chapter two discusses the general NIL process as well as several possible variations of NIL. It also goes over material selection issues and discuss approaches for experiments. Chapter three covers the experimental details of the imprint process that was selected for this thesis. Two sets of imprint process at different size scales are included. Chapter four discusses the results of the two sets of experiment. Results contain images and measurements with optical microscope, Scanning Electron Microscopy (SEM), Atomic Force Microscopy (AFM), and Ellipsometry.

CHAPTER TWO: METHODS

In this chapter the working principles and different implementations of Nanoimprint lithography and Soft UV Nanoimprint lithography are discussed. In addition, approaches and materials used in this report, from mold fabrication to resists, are discussed as well.

2.1 The Working Principle of Nanoimprint Lithography

Since the first Nanoimprint Lithography experiments were published by Chou *et al.* in 1995[29], the method of nanoimprinting has been widely discussed and researched. Many different methods have been proposed for doing nanoimprinting. In general, Nanoimprint lithography can be separated into two classes: one is Thermal Nanoimprint Lithography; the other is UV Nanoimprint Lithography. The main difference between these two methods are the way to pattern resist layer, which will be discussed below.

2.1.1 Thermal Nanoimprint Lithography (T-NIL)

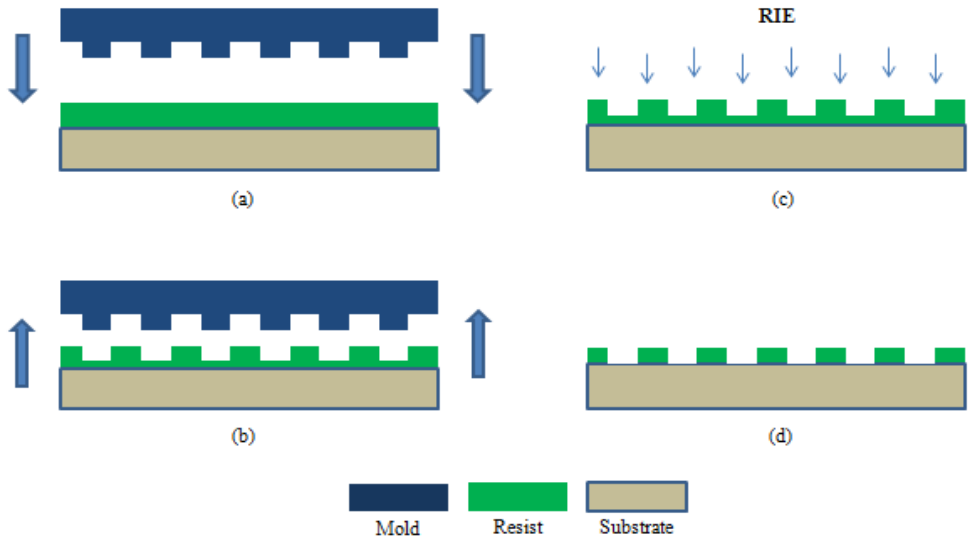

Figure 2. Schematic illustration of Thermal Nanoimprint Lithography.

When transferring patterns from master mold to resist layer, the resist needs to be able to flow and fill up all the cavities of the master mold in order to obtain exact replicas of the original patterns. One way to achieve this is to soften and re-shape solid-phase polymer resist thin films by applying high temperature and high pressure in a process called Thermal Nanoimprint Lithography, or T-NIL. In T-NIL, there are three basic components: a patterned mold, a thermo-elastic resist thin layer, and a substrate. Since the processing environment of T-NIL is high temperature (~180^{o}C) and high pressure (~200 psi), materials for mold and substrate need to be able to endure these processing conditions. The imprint mold should be a hard material and have a high melting point, for example, SiO_2 or Si, in order to have enough

toughness to imprint into the resist layer under high temperature without deforming. The mold needs to be prepared through other lithography techniques, for example, EBL, and treated with anti-sticking agent, such as Trimethylchlorosilane (TMCS), to prevent the mold from getting stuck to the resist The T-NIL resist should be a thermo-elastic polymer which can be softened when the temperature is above its glass transition temperature (T_g), for example, Poly(methyl methacrylate) (PMMA). The substrate can be varied to meet different purposes as long as it can support the resist layer during imprinting process and handle the high processing temperatures used. Typical substrates are glass or silicon.

The procedure of T-NIL is described in Figure 2: (a) sample heating, applying pressure, and imprinting. When the temperature is increased above the resist's glass transition temperature (T_g), the hardness of resist will drop, and the patterned mold can be pressed into the resist layer by applying additional pressure on the mold. During imprinting, the resist layer will be re-shaped according to features on the imprint mold. While the imprint mold is held against the substrate, the temperature is reduced to below T_g causing the solidification of the resist; (b) Mold separation and (c) pattern transfer. Generally, the imprint step can leave a small amount of residual resist in the recessed areas. This would lead to a problem in the lift-off process. To remove this unwanted residual resist and expose the substrate, often a plasma clean or

Reactive Ion Etching (RIE) pattern transfer step is used. After pattern separation a patterned resist coated substrate is obtained (d). Imprinted samples are then further processed e.g. with material deposition or etching to obtain the intended nano-structures.

The process of T-NIL is straightforward and the resolution of it can be high (sub-20 nm feature sizes have been achieved[30]). However, since T-NIL is a high-temperature and high-pressure process, the choice of materials is somewhat limited.

2.1.2 Ultraviolet Nanoimprint Lithography (UV-NIL)

Ultraviolet Nanoimprint Lithography (UV-NIL) is another approach to NIL that was first proposed by Haisma *et al.* in 1996[31]. Instead of imprinting into a high-T_g resist layer, UV-NIL imprints into a low-viscosity polymeric resist layer that is hardened by UV-curing during the imprint step. UV-curing of polymers is a chemical reaction that causes polymer molecules (usually in liquid phase) to crosslink with each other through the help of free radicals that are released by photo-initiator molecules in the resist upon absorbing UV photons. Cross linked polymers contain chemical bonds between adjacent polymer strands, which hardens and solidifies the resist.

The components used in UV-NIL are similar to T-NIL: mold, resist and substrate, but in this case the materials of these component and the processing environment can be quite different since UV-NIL relies on UV curing rather than high temperature. The process of UV-NIL can be done at room temperature and at low pressure. Therefore, heat-resistance is not a requirement for the materials used in UV-NIL. However in this case, at least one component , either mold or substrate, should be transparent to UV radiation. For the mold, in addition to traditional SiO_2 or silicon molds, lower T_g materials can also be used, such as polydimethylsiloxane (PDMS) and PMMA, as discussed in the next section. The resist can be a commercial UV-curable resist[32,33] or can be mixed based on basic constituents[34].

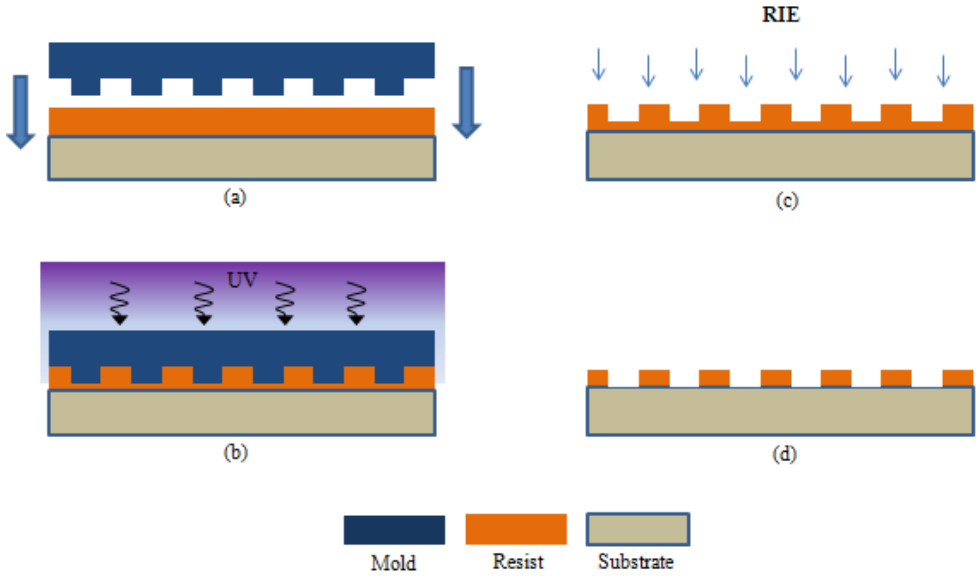

Figure 3. Schematic illustration of Ultraviolet Nanoimprint Lithography.

Figure 3 describes the procedure of UV-NIL: (a) Imprinting and (b) UV-curing. When the patterned mold is pressed into the liquid resist film, the resist can easily re-distribute and fills up cavities of the mold. While the imprint master and the substrate are in contact UV light is applied to solidify the molded resist. (c) Separation and pattern transfer: after resist curing, the mold can be separated from the resist film, typically followed by reactive ion etching (RIE) to remove any residual resist in the depressed regions, resulting in complete pattern transfer of the designed patterns into the resist layer (d). After imprinting and RIE, the sample can be processed with materials deposition or etching to obtain patterns with different materials.

Compared to T-NIL, UV-NIL is compatible with a larger number of mold and resist materials. UV-NIL also has a more friendly processing environment (low temperature and pressure) compared to T-NIL. In addition, since UV-NIL can make use of low T_g and relatively soft materials, it can be applied on non-planar surfaces, for example, curved surfaces[35], to meet different purposes. The resolution of UV-NIL can also be very high (sub-30nm feature size has been reported).[36].

2.1.3 Bilayer Imprint Method

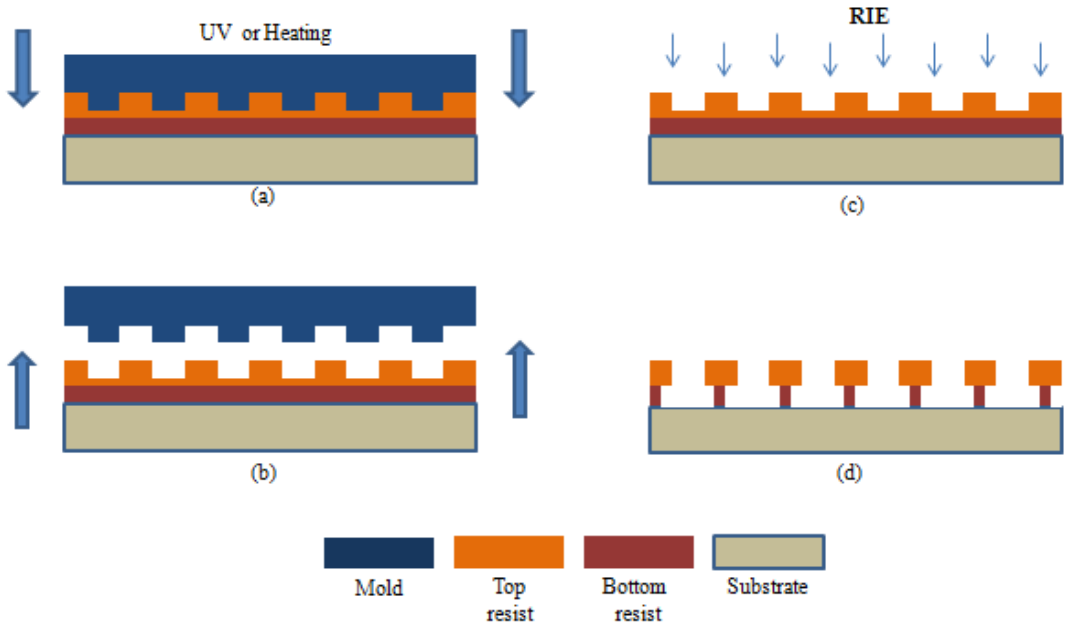

Figure 4. Schematic illustration of Bilayer Nanoimprint Lithography

When NIL is used for the generation of metallic nanostructures, the imprint step is typically followed by vacuum deposition of metal onto the patterned sample, followed by lift-off. However, the single layer of resist used in both T-NIL and UV-NIL may be problematic when doing metal deposition and lift-off. If the imprint process leaves sidewalls that are not perfectly vertical, metal may end up being deposited on the non-vertical sidewalls, form a continuous metal film on the sample, as shown in Figure 5(b), which causes detachment of the metal nanostructures during the lift-off process[37]. Non-vertical sidewalls happen in imprinting process if the imprinting mold does not have patterns with vertical sidewalls, or if the imprinted resist deforms or re-flows slightly during or after the mask separation. Non-

vertical sidewalls can also result from a RIE step for residual resist removal, if the RIE process is not sufficiently directional.

A method was proposed to overcome this challenge: Bilayer Nanoimprint lithography[37]. This method had been proposed on both T-NIL[37] and UV-NIL[38]. The procedure of bilayer imprint is presented in Figure 4. It is similar to T-NIL and UV-NIL but makes use of an additional bottom resist layer in the structure. The main purpose of the additional bottom resist layer is to facilitate material deposition and lift-off. In bi-layer NIL, these resist layers are typically made of different materials that have different etch rates in RIE, with the top layer having the lower etch rate. Therefore, top layer is etched more slowly than the bottom layer during the certain RIE process. The difference in etch rates results in an undercut bilayer resist structure[37] on the substrate after RIE, as shown in Figure 5(c).

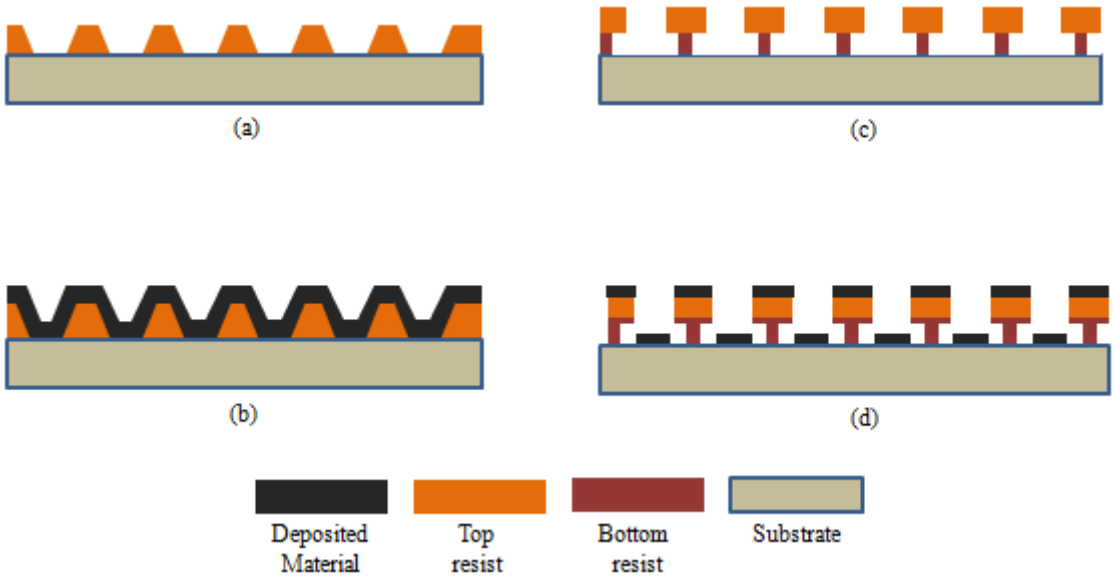

Figure 5. Comparison of deposition situations between non-vertical sidewall structures and bilayer undercut structures.

When depositing materials on bilayer undercut structures, materials are deposited all over the surface, but they end up either sitting in the windows between undercut structures and on top of the undercut structures, forming discrete separated patches on the surface of sample, as presented in Figure 5(d); which prevents deposited features from being torn or detached during the lift-off process.

2.2 The Working Principle of Soft UV Nanoimprint Lithography

Based on the previous sections it seems that bilayer UV-NIL enables low-cost reliable nanopattern replication. However, one important challenge remains: during NIL as described previously, medium to high pressure physical contact is needed between the patterned mold and the resist layer. This can lead to damaging of the delicately patterned high-cost hard

master molds. To avoid this problem, a modified version of UV-NIL, namely Soft UV-NIL has been proposed. Soft UV-NIL uses a flexible transparent polymer mold typically made of PMMA, PDMS, or PVA that can be used to replicate a hard negative master mold in a low-pressure process that does not involve the pressing together of two hard materials. This minimized the chance of damage to the hard master mold. The flexible and polymeric mold has the advantage of easy low-cost fabrication, UV transparency, and commercial availability of the materials needed. A tri-layer mold is typically used in Soft UV-NIL[39,40,33] consisting of a thin top layer, a softer and relatively thick middle buffer layer, and a glass supporting substrate (bottom). The top layer will contain the replicated patterns from the hard master mold and is usually made of polymer with a higher Young's modulus, such as PMMA, H-PDMS, or PVA, in order to have enough strength to support ultra-small (sub-100nm) features. PDMS (Sylgard 184 or RTV615) is commonly used in middle layer; due to PDMS's low Young's modulus, middle layer is softer than top layer and it serves as a buffer layer that allows conformal contact with the final sample even at low imprint pressure. The bottom glass substrate supports handling and processing of the generated soft mold and minimizes mold distortion.

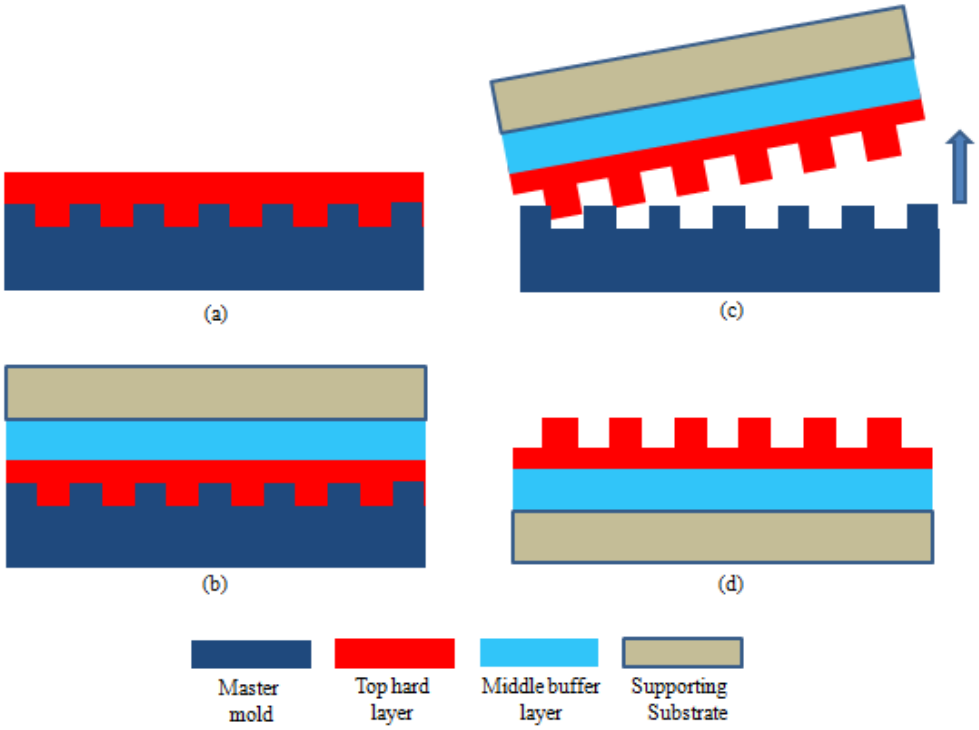

Figure 6. Schematic illustration of soft mold fabrication process.

The process of the soft mold fabrication is quite straight forward, as presented in Figure 6. First, (a) The nanostructured hard master mold is coated with an anti-sticking layer followed by spin coating of a polymer solution onto hard master mold to form the top layer of the soft mold. The low viscosity of this layer allows filling of the nanostructures in the master mold. This is followed by a baking process to cure the polymer, leaving a solid film on top of the mater mold. Second, (b) PDMS is poured on the top layer to form the middle buffer layer followed by thermal curing of the PDMS and placing a glass substrate on the PDMS layer before PDMS is fully solidified as a mechanical support. After (c) separating the tri-layer soft

mold from master mold, (d) a tri-layer soft mold is obtained, ready to be used as a soft mold. This soft mold can be used subsequent UV-NIL experiments.

A resolution of 20nm scale for Soft UV-NIL has been achieved[41] and a real-world application of Soft UV-NIL has also been reported[21] involving the generation of large-area localized surface plasmon resonance based sensors. Based on the discussion above, soft UV-NIL combined with the trilayer resist approach promises to allow cost-effective replication of nanoscale patterns with minimal risk of damage to the hard master mold and good performance in the lift-off process. Therefore, in this report, a Soft UV-NIL process is developed as a nanofabrication tool to produce plasmonic antenna arrays.

2.3 Approaches and Materials Discussion

The previous sections introduced the principles several NIL approaches. In this section, the procedure and materials that are used in this report are presented and discussed. There are two parts in this section. The first section focuses on the imprint process used in this report. The second part discusses the materials chosen for each steps in the imprint process.

2.3.1 Approaches

The goal of this report is to achieve the fabrication of metallic antenna arrays using soft UV-NIL combined with Bilayer NIL.

The first experiments will use low-resolution structures to test the overall imprint process. This will be followed by nanometer-scale imprint experiments using the same materials, but with adjusted layer thicknesses suitable for nanoscale feature replication. We first describe the soft mold fabrication, then the imprint process using the soft mold, and finally, metal deposition and lift-off. For clarity the entire planned process, consisting of soft mold generation and the bilayer imprint step are summarized in Figure 7. Soft mold fabrication: (a) spin coating of the top hard layer on a master mold; (b) applying the buffer layer and the supporting substrate (optional); (c) separating the cured soft mold from the master mold; (d) coating the surface of the soft mold with anti-sticking agent. Imprint process: (e) Imprinting the soft mold on a bilayer resist and UV-curing; (f) separating the soft mold from the cured bilayer resist; (g) transferring the imprinted pattern using RIE; (h) the resulting undercut patterns. Metal deposition: (i) deposit the desired metal using thermal evaporation; (j) the final plasmonic metal antenna array after lift-off. In each part, the results will be inspected by Atomic Force Microscope (AFM). Finally, the metal array will be measured for its optical response. The experimental details will be presented in Chapter 3: Experiments.

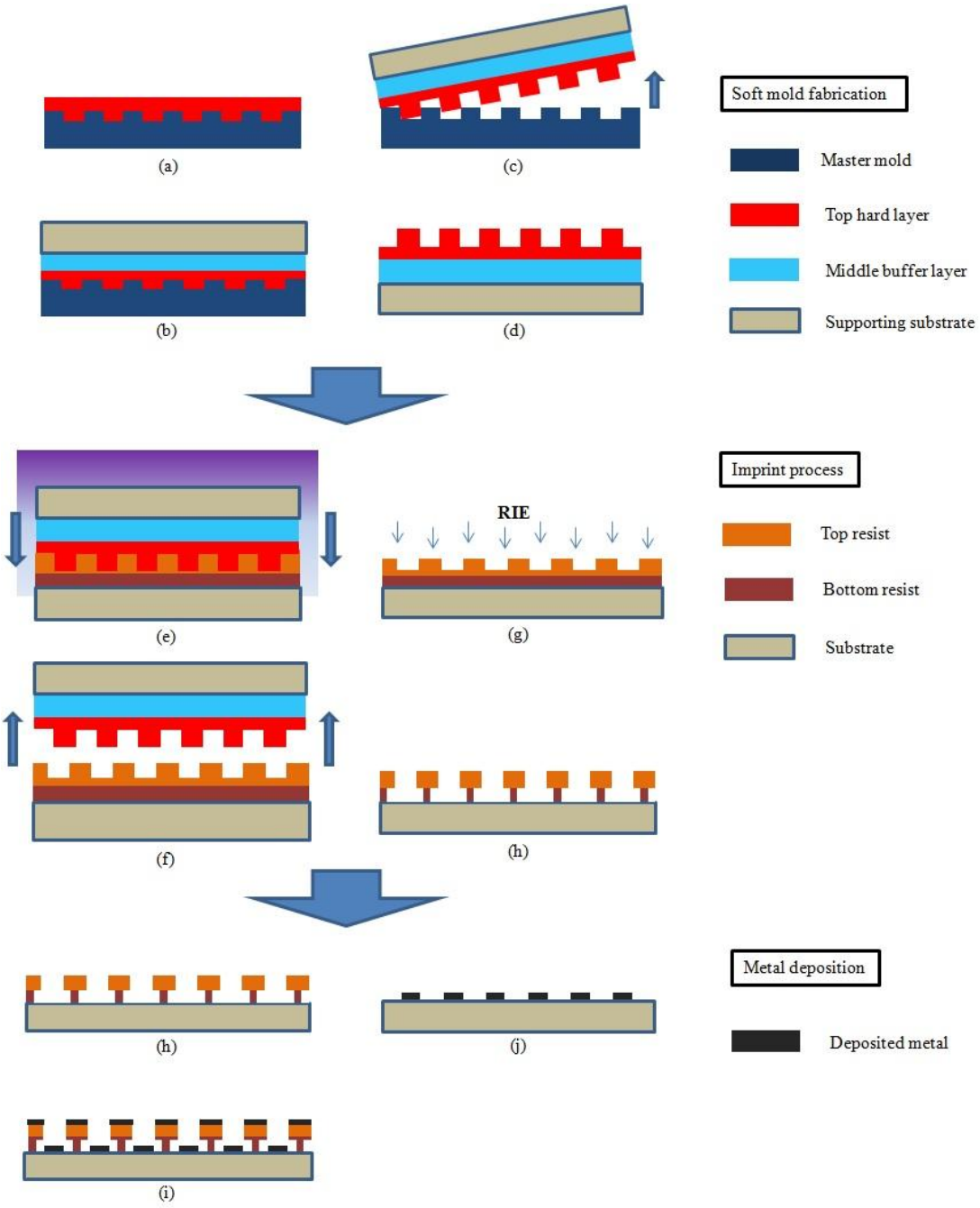

Figure 7. Schematic illustration of the entire process of bilayer Soft UV-NIL used in this report

2.3.2 Material Selections

In this report, two full Soft UV-NIL processes are attempted, namely a micrometer-scale test imprint and a nanometer-scale imprint process. Each full process includes many steps where materials need to be chosen. The following describes the various material choices that have been made.

2.3.2.1 Materials for Molds

The low-resolution master mold in the test imprint is made of a glass slide coated with a 1.5μm SiO_2 layer. Glass slides can be easily cleaned and are commonly used as a substrate in optical experiments. In order to have the low-resolution glass master mold with 1μm feature depth, CF_4 RIE is used to etch the glass slide. However, since normal glass slide has very high resistance to CF_4 RIE (5nm/min measured), it takes a long time for RIE to etch 1μm depth features on normal glass slide. Therefore, an additional SiO_2 thin layer, which has higher etch rate (30nm/min) is deposited on the glass slide to facilitate the pattern transfer process in RIE. The negative nanometer-scale master mold was provided by Prof. Debashis Chanda (NanoScience Technology Center, UCF). The patterns are fabricated on a spin-on-glass layer on top of glass slide.

The materials used for the tri-layer soft mold were the same in both micron scale and nanometer-scale imprint processes. A simple tri-layer structure is shown in Figure 8(a). In this report, PMMA, H-PDMS, and PVA are considered for the top hard layer; commercial PDMS (Sylgard 184) is used for middle buffer layer; and glass is used as a supporting substrate. Chemical structures of these polymers are shown in Figures. 8 (b),(c),(d). The reasons for using these polymers are as follows:

PMMA has a Young's modulus between 1.8 and 3.1 GPa and is has successfully be used in Soft UV-NIL.

H-PDMS[42] *(Hard-PDMS):* it consists of a mix of pre-polymer, Vinylmethylsiloxane-dimethyl-siloxane (VDT-731, Gelest), hydrosilane pre-polymer, Methylhydrosiloxane (HMS-301, Gelest), catalyst, Platinum divinyltetramethyldisiloxane (SIP6831.2LC, Gelest), and modulator 1, 3, 5, 7 tetramethyl cyclotetrasiloxane (SIT-7900, Gelest). This combination of polymers achieves a hardness that is four times larger than of commercial PDMS (Young's modulus of 1.8 MPa), and is therefore called Hard PDMS (H-PDMS). This material has been widely used in Soft NIL.

PVA is a water soluble polymer with a Young's modulus 1.9GPa[43] similar to PMMA. Also, PVA is resistant to organic solvent, oil, and grease. Meanwhile, it has been observed that processes using PVA molds exhibit better mold-resist separation than PMMA molds. Therefore, PVA is also considered as a candidate for the top layer in the soft mold.

PDMS (Sylgard 184) is a well-known polymer that is widely used in many applications. Its low Young's modulus allows conformal contact, making it a good buffer between the top hard layer and the handle substrate.

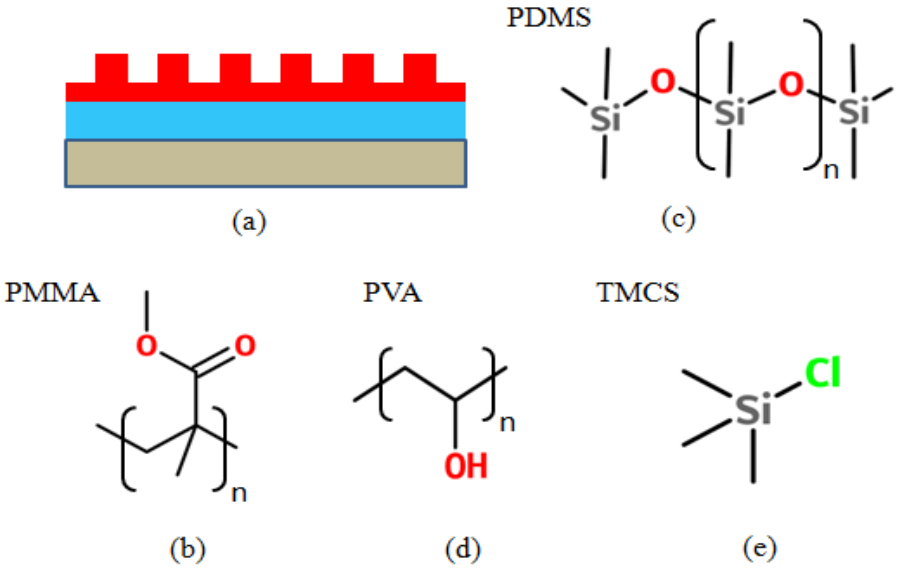

Figure 8. (a) Demonstration of tri-layer soft mold. Chemical structure of (b)PMMA, (c)PDMS, (d)PVA, (e)TMCS

As a mold releasing agent or anti-sticking layer trimethylchlorosilane (TMCS) and liquid self-assembled monolayer (SAM) from Minuta Technology, Korea, were used. TMCS can be

applied by vapor deposition, forming a self-assembled monolayer on the surface, which can lower the surface energy of the target surface, protecting the target surface layer from sticking to other materials. Liquid SAM from Minuta can be applied by spin coating and serves a similar purpose to TMCS but uses a different type molecule to form the SAM[44].

2.3.2.2 Materials for Resists and Substrate:

In the bilayer method, the top layer is not only a pattern defining area but also serves as an etching mask in the pattern transfer process. Therefore, the materials for the top resist layer in this report should be both UV-curable and highly etch resistant to the pattern transfer process, which is oxygen (O_2) RIE in this report. A custom-mixed M-PDMS based UV-curable resist was used as the top resist layer.

M-PDMS based UV-curable resist: This resist consist of methacryloxypropyl terminated polydimethysiloxane (DMS-R05, Gelest Inc.), Irgacure 184, and methacryloxtpropyl-trichlorosilane (SIM6487.2, Gelest Inc.). The chemical structures of these chemicals are listed in Figure 9. M-PDMS is the base resist; Irgacure 184 is a photoinitiator which will release free radicals to upon absorbing UV light. SIM6487.2 is an adhesion promoter for resist and substrate.

As a UV-curable resist, M-PDMS has several advantageous properties. The first is that the PDMS contains methacrylate terminating groups. Methacrylate groups allow the M-PDMS molecule to be cross-linked with the help of free radicals. Second, because the Si compounds in M-PDMS will be oxidized to SiO_2 when interacting with oxygen ions, a thin layer of SiO_2 will be formed on the surface of M-PDMS layer during O_2 RIE; this property gives M-PDMS based resist a very high resistance to O_2 RIE[34][In addition, these materials are low cost compared to commercial UV-curable resists.

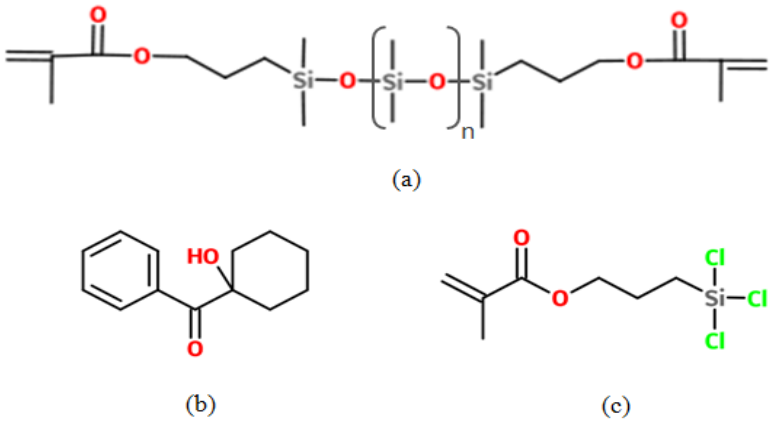

Figure 9. Chemical structures of (a)Methacryloxypropyl terminated Polydimethy-siloxane, (b) Irgacure 184, (c) Methacryloxtpropyl-trichlorosilane.

The bottom layer resist: *PMMA* is used as the bottom layer in the bilayer resist since PMMA has good adhesion to common substrates like silicon or glass substrates, and is very easy to apply and remove. In addition, PMMA has a very high etch rate in O_2 RIE which is necessary to achieve the desired undercut in the RIE pattern transfer process. PMMA is commonly

provided in powder. PMMA in powder form can be dissolved in anisole to enable spin-coating. To achieve thin layers, a dilute solution of PMMA in anisole is used.

Glass cover slips and silicon wafers are used as imprint substrate in this report. Both materials are rigid, optically flat, and easy to handle. Since the soft mold is glass-backed and UV transparent, the use of a non-transparent Si substrate is possible in the UV-NIL process.

CHAPTER THREE: EXPERIMENTS

This chapter discusses the experimental procedures and results obtained. Most experiments were done in CREOL's cleanroom (R210) and in the NanoPhotonics and Near-field Optics Group's laboratories. The imprint process was done on NX2500, Nanonex, managed by Prof. Hyoung Jin Cho's group, in the cleanroom of Engineering I. There are two main experiments in this report: micon-scale test imprint and nano-scale imprint.

3.1 Master Mold Fabrication

For the low-resolution test imprint, a master mold was prepared using laser writing. Patterns for the test imprint were designed using AutoCAD. The overall image of the designed patterns (micron-scale) is shown in Figure 10. There are three main pattern areas on the test mold and three pattern blocks in each main area. Feature sizes and shapes were designed to vary from area to area in order to test the capabilities of Soft UV-NIL in replicating different kinds of features. The first area is a *lines area* which has lines with various width and spacing ranging from 5μm to 15μm. The second area is a *shapes area*, containing triangles, L-shapes, circles and squares with different sizes ranging from 3μm to 10μm. The third area is a *contrast area* containing square features with different aspect ratios. Numbers (around

700μm in size) were included to in the middle of each pattern block indicate the size of each block and as a locator when using a microscope for visualization.

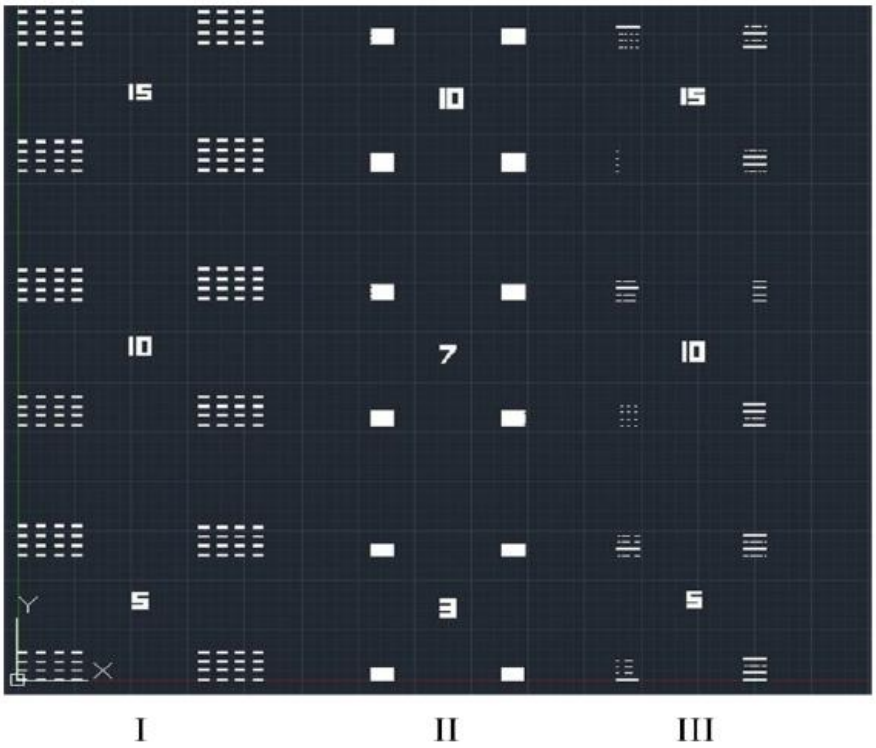

Figure 10. Overall image of designed pattern of master mold for test imprint.

Next, laser writing technique was performed to transfer the designed patterns to a Chromium (Cr) photomask. The patterned photomask was used subsequent photolithography. For laser writing, photoresist S1805 was spin-coated onto a Cr photomask and pre-baked for 30 minutes. Then designed pattern was imported and the photomask was sent to the laser writer. The photomask was exposed by UV laser (λ=426nm) direct writing. After laser writing and a 30-minute post-bake, the photomask was developed to remove the exposed resist followed by

wet etching to remove Cr under the exposed and developed regions. The thus obtained patterned photomask can be used in photolithography.

Before doing photolithography, a thin layer (1μm) of SiO_2 was deposited on a clean glass slide, which will act as the un-patterned master mold, via Plasma-Enhanced Chemical Vapor Deposition (PE-CVD). The deposition conditions are listed in Table 2. After SiO_2 deposition and cleaning, photoresist, NR7-1000P was spin-coated on the SiO_2 coated substrate. Then photolithography was performed using the Cr photomask made by laser writing. The recipe of applying NR7-1000P is listed in Table 1.

Table 1. Recipe for Photolithography using NR7-1000P negative photoresist.

Resist	Spin-coat	Pre-bake	UV-exposure	Post-bake	Develop
NR7-1000P	4000rpm, 40s	150^{o}C,1mn	5s	100^{o}C, 1min	11s

Subsequently CF_4 RIE was used to transfer patterns in to SiO_2 layer. However, since photoresist is not a good etch mask in CF_4 RIE when the etch depth is large, a thin layer of Cr was thermally evaporated onto the patterned SiO_2 substrate as an etch mask. After lift-off of the deposited Cr, a 35 minute RIE step was used to transfer the patterns into SiO_2 layer. The etch condition of CF_4 RIE is listed in Table 2. Then the Cr layer was removed by wet Cr etching, leaving clean and well-defined features on the SiO_2 layer to be used as a hard master mold

Table 2. Recipes for SiO2 deposition and etching.

Type	Gas	Pressure	RF power	DC bias	Time	Rate
SiO2 deposition	SH_4 400sccm NO_2 826sccm	1052 mTorr	24W	5V	30mins	45nm/min
SiO2 etching	CF_4 45sccm	100 mTorr	174W	381V	35mins	30nm/min

3.2 Anti-sticking Treatment

Before preparing the soft mold, master molds were treated with anti-sticking treatment. Liquid SAM developed by Minuta, Korea, was spin-coated on the master mold at 3000 rpm for 30 seconds and then baked at 105^{o}C for 12 hours. In addition, an alternative method for applying the anti-sticking layer has been tried in this report: TMCS vapor deposition. To apply TMCS, the master mold and 1-2 mL of TMCS were placed in a 150mm petri dish in a Fume hood for 30 minutes.

Figure 11 presents an example of the result of the anti-sticking coating. Normally, an anti-sticking layer coated surface has low surface energy. Drops of water were placed on two cover slips, one of which was coated with anti-sticking agent. The results are strikingly different as a result of the surface modification: the top substrate is anti-sticking coated, and droplets are seen to have a large contact angle with the glass substrate, a clear indication that the substrate is hydrophobic; the bottom substrate is not anti-sticking coated, and shows droplets that have a significantly lower contact angle.

Figure 11. Comparison of anti-sticking coated (top) and uncoated (bottom) cover slips

3.3 Soft Mold Fabrication.

When the anti-sticking treatment was completed, the master mold was ready for soft mold fabrication. Soft mold fabrication started with top hard layer materials mixing. Then the mixed polymer solutions were spin-coated onto the master mold and cured at specific temperatures. Three kinds of polymers were used for the top hard layer: PMMA, PVA, H-PDMS. Each polymer had its own contents, mixing method, and application method, which are listed in Table 3.

After curing the top hard layer, a 10:1 PDMS mixture was degassed in low vacuum for 20 minutes. Then the PDMS mixture was poured on top of the top hard layer and baked at 80^{o}C for 1 hour. Note that if a supporting substrate is used, it should be placed on top of PDMS after 5 minutes of baking at 80^{o}C, otherwise the PDMS may flow out due to the weight of the supporting substrate.

When all layers were cured, the soft mold was manually separated from master mold and treated with anti-sticking agent using the same method above. The layer thickness of top and middle layer were approximately 5 μm to 10μm and 1 mm to1.5 mm, respectively, as measured by Profilometer.

Table 3. Recipes for making top hard layer and middle buffer layer of tri-layer soft mold.

Materials	Contents	Mixing methods	Applying methods
PMMA	15 wt% PMMA 85 wt% Anisole	1. Weight 15wt% PMMA and 85% Anisole 2. shake the mixture for 2-5 minutes. 3. Wait for 24 hours until all PMMA are dissolved.	1. Spin-coat at 1500rpm for 40 second. 2. Bake at 180^{o}C for 1 hour.
H-PDMS	1.7g of VDT-731 0.5g of HMS-301 9μL of SIP6831.2LC 2.2μL of SIT-7900	1. Weight 1.7g of VDT-731, 2. add 9μL of SIP6831.2LC and 2.2 μL of SIT-7900 in VDT-731 then stir it. 3. Degas for 2-3 minutes. 4. Add 0.5g of HMS-301 then slowly stir the solution.	1. Spin-coat at 1500rpm for 40 seconds. 2. Bake at 65^{o}C for 1 hour.
PVA	10 wt% PVA 90wt% Water	10 wt% PVA solution, bought from Bostick & Sullivan Inc	1. Spin-coat at 1000rpm for 30 second 2. Degas in vacuum for 10 minutes. 3. Bake at 105^{o}C for 30 minutes.
PDMS	10 parts of Sylgard 184 A (polymer) 1 part of Sylgard 184 B (curing agent)	1. Weight 0.5g of Sylgard 184 B and 5g of Sylgard A. 2. Degas in vacuum for 20 minutes.	1. Pour a desire amount of top of top hard layer. 2. Bake at 80^{o}C for 1 hour.

3.4 Bilayer resist application

This section describes the application of the bilayer resist on the substrate. First, to apply the PMMA bottom layer a 5% PMMA solution in anisole was spin-coated on substrate at 4000 rpm for 40 seconds and baked at 180^{o}C for 2 minutes to evaporate its solvent, which resulted in a 300nm PMMA bottom layer. Then, the top layer resist, M-PDMS based UV-curable resist, was spin-coated at 7500rpm for 90 seconds for nanoimprint, and 5500rpm for 90 seconds for the test imprint. No pre-bake is needed for this layer. Once the two layers were spin-coated on the substrate, the soft mold was then placed on top of resist substrate. The whole combination was stored in an air-tight, black box and brought to the Engineering I cleanroom, where the nanoimprint machine, NX2500 is located.

3.5 Imprint on NX2500

The nanoimprint machine (Nanonex NX2500) utilizes Air Cushion Press (APC) to apply uniform air pressure up to 500psi to every dimension. It has a 200W broad band (320-390nm) UV lamp for in-situ resist curing.

The condition of the imprint process is listed in Table 4. Before the imprint, the imprint chamber was evacuated to 14 psi below atmospheric pressure for 2 minutes, which can expel

oxygen to prevent oxygen inhibition. The system then increases the pressure and reaches the set temperature (close to room temperature in the UV-NIL process) and set pressure for 2 minutes process time; during the process time, the UV-resist is re-distributed by the applied pressure. Then, the system starts UV illumination for 10 minutes to cure the resist. After imprinting, the sample was taken back to CREOL's upstairs cleanroom using the same method above. Mold-resist separation was done by inserting a knife or sharp tweezers at the edge of the sample and slowly separating the imprint mold and the bilayer resist-coated substrate.

Table 4. Imprint condition of soft UV-NIL done one NX-2500.

Type	Vacuum time	Temperature	Pressure	Process time	UV-on time
UV imprint	2 minutes	25^{o}C	20 psi	2 minutes	10 minutes

3.6 RIE Pattern Transfer and Metal Deposition

To complete the processes RIE pattern transfer, metal deposition, and lift-off were carried out. There were two steps of RIE: CF_4 and then O_2 RIE. CF_4 RIE was used to remove residual resist layer, which was around 150nm thick; and O_2 RIE was for transferring pattern and creating the undercut structure on substrate. The recipe of both RIE steps are listed in table 5. When RIE processes were completed. 60 nm Cr was deposited on the sample via thermal evaporation. Lift-off was done by sonicating the sample in Acetone for 2 minutes.

Table 5. Recipes for RIE pattern transfer steps.

Type	Gas	Pressure	RF power	DC bias	Time	Rate
CF_4	CF_4 45sccm	100 mTorr	175W	285V	2 mins	100nm/min
O_2	O_2 75sccm	100m Torr	299W	481V	2 mins	>10nm/sec

CHAPTER FOUR: RESULTS

This chapter describes the results of the nanoimprint experiments as well as the spectral measurements on the replicated patterns. The imprint results include a low resolution test imprint and nanoimprint of a mask with sub-micron feature sizes.

4.1 Test Imprint Results

4.1.1 Mold Fabrication: master mold and soft mold.

In the low-resolution test master mold fabrication (see Section 3.1) the shapes of some features, especially small (<5um) features, were slightly different from the designed shapes. Figure 12 shows the images of 50X Bright field optical microscopy of the test master mold after etching. The observed uneven lines were designed to be straight lines with uniform width and with fixed inter-line spacing. The observed deviations from their designed shape is attributed to intrinsic defects of the laser writing process when patterning small features. The depth of features after 35 minutes of SiO_2 RIE was measured to be 1000 ± 10nm. This confirms that the etch rate of SIO_2 RIE on deposited SiO_2 layer is 30nm per minute.

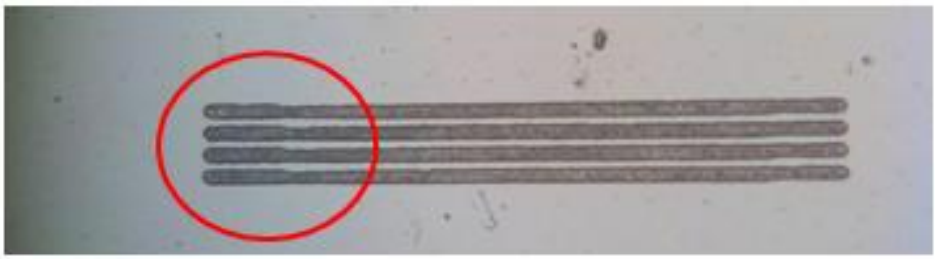

Figure 12. Uneven Lines features on fabricated low resolution test master mold.

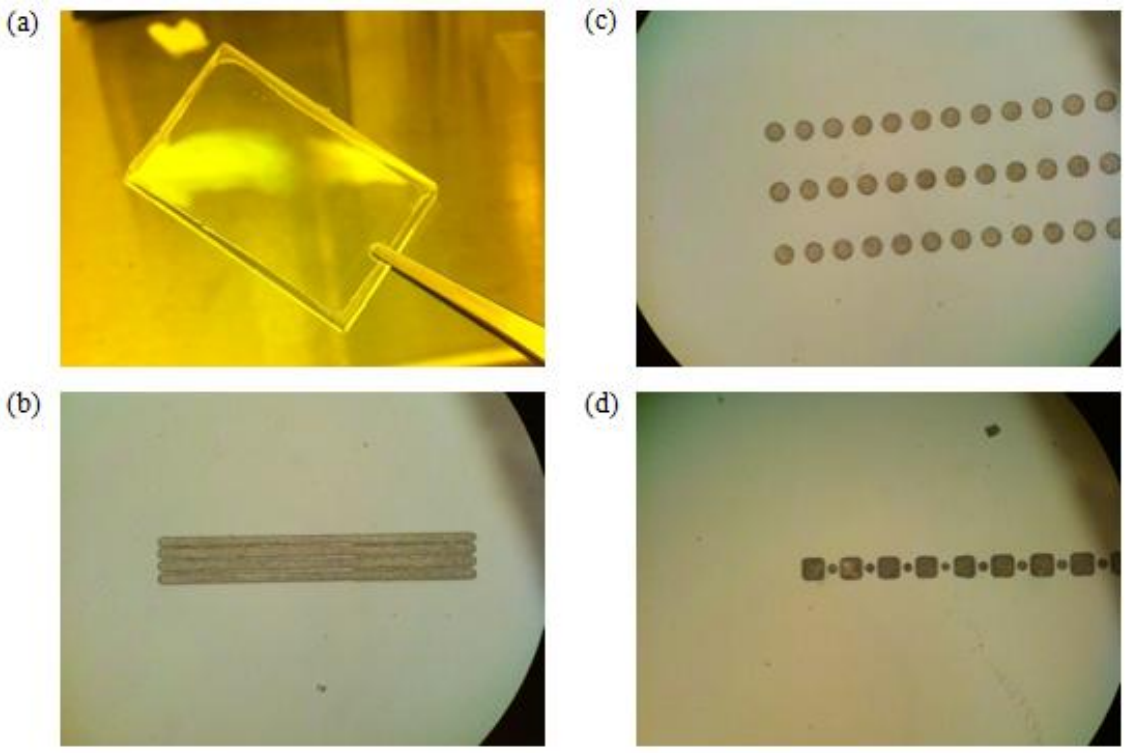

Figure 13. PMMA low-resolution soft mold (a) Top view of PMMA low-resolution soft mold. (b)Features in lines area (c) Features in shapes area. (d) Features in contrast area. All features are ~10μm in size, pictures were taken under 50X microscope.

Although the test master mold contains some deviations from the original design, the patterns including their imperfections should be transferred to the soft mold, and thus this mask can serve as a good replication test. In the soft mold fabrication, all soft mold materials: PMMA,

PVA, and H-PDMS, were successfully used to replicate the test master mold. Figure 13 shows different areas of the obtained patterned PMMA soft mold, held on a PDMS layer on the glass backing substrate. Since all layers of the soft mold are transparent in UV and visible range, the mold looked perfectly optically clear and is expected to be suitable for UV-NIL. Features on every area of the designed pattern were successfully replicated in the soft molds (Figure 13(b)(c)(d)), as will be shown in more detail below. The height of features as measured using an Alpha Step 200 profilometer were found to be 1000nm±10nm which corresponds to the depth of the features on the master mold. The height of features was found to be consistent for all soft molds including the mold with the PVA hard layer and the mold with the H-PDMS hard layer, showing that all soft mold materials have the ability to replicate features as small as 5μm, and possibly smaller. One important point to note is the need to prevent bubble formation in the soft mold fabrication. Bubbles may be trapped or formed during the curing of the PDMS buffer layer due to the presence of residual solvent vapor from the top hard layer. Figure 14(a) shows typical bubble-containing soft mold. These bubbles may greatly affect the imprint results. For example, in Figure 14(b), the features indicated by the arrow were totally eliminated by the presence of a large bubble (dark faint circular outline) after imprinting at 35psi for 10mins (bottom figure). Therefore, it's important to prevent any bubble from being trapped or formed during soft mold fabrication.

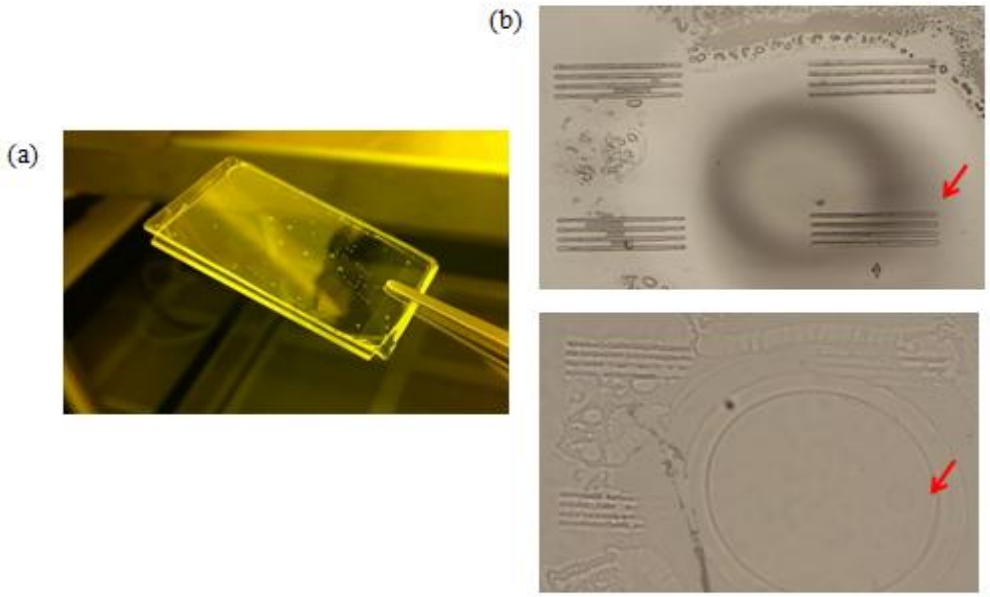

Figure 14. Influence of bubbles on imprinting. (a) bubble-trapped soft mold. (b) bubble-trapped soft mold (top figure), and corresponding imprint result (bottom figure).

4.1.2 Soft UV-NIL Results.

For the bilayer imprint step with the soft molds obtained from the test master mold, two layers of resist were spin-coated on a glass substrate: first a PMMA layer was spin coated, followed by the spin coating of an M-PDMS based UV-curable resist layer using the settings shown in Section 3.4. The thickness of the PMMA bottom layer was 300nm $\pm$ 5nm as measured by profilometer and the top UV-curable resist layer had a thickness of ~470nm as measured by Variable Angle Spectroscopic Ellipsometry (Woollam M2000). The UV-curable resist layer thickness was obtained by fitting the ellipsometry data by modeling the thin film on glass as a Cauchy layer with a dispersion of the form $n(\lambda) = A + \frac{B}{\lambda^2} + \frac{C}{\lambda^4}$. The best fit

was obtained by a Cauchy model with a thin film refractive index, n, of 1.489 at 632.8nm. This is higher than the known refractive index of pure M-PDMS of 1.416, suggesting that the addition of the photoinitiator (Irgacure, refractive index 1.571) and the adhesion promoter (refractive index 1.465) increased the thin film index. The fitting result is shown in Fig. 15 and Table 6.

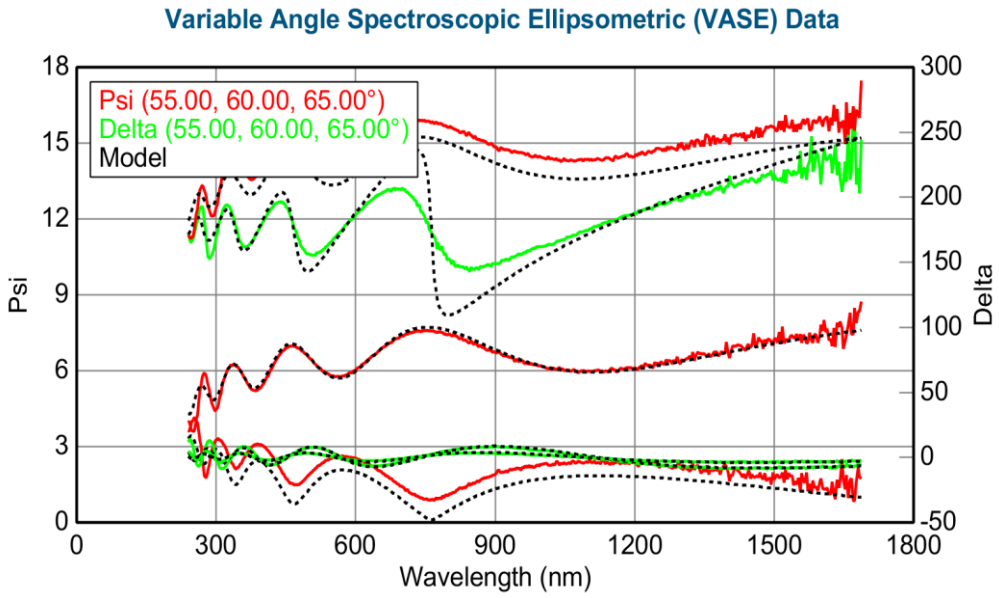

Figure 15. Ellipsometry fitting result for UV-curable resist after spin-coating at 5500rpm for 90 seconds.

Table 6. Fitting parameter for M-PDMS UV resist spin coated at 5500rpm.

MSE	Roughness	Thickness	A	B	C
12.018	0.55 ± 0.399 nm	466.10 ± 2.689 nm	1.474 ± 0.00072701	0.00596 ± 0.00031096	-4.5802E-05 ± 2.2186E-05

After bilayer resist thickness determination, the UV imprint process was done on a Nanonex NX2500 NIL system using the conditions listed in Table 4. The separation of the mold and bilayer resist coated substrate was successful using PMMA and PVA molds. The imprinted features are compared with the original features on master mold and the soft mold in Figure 16.

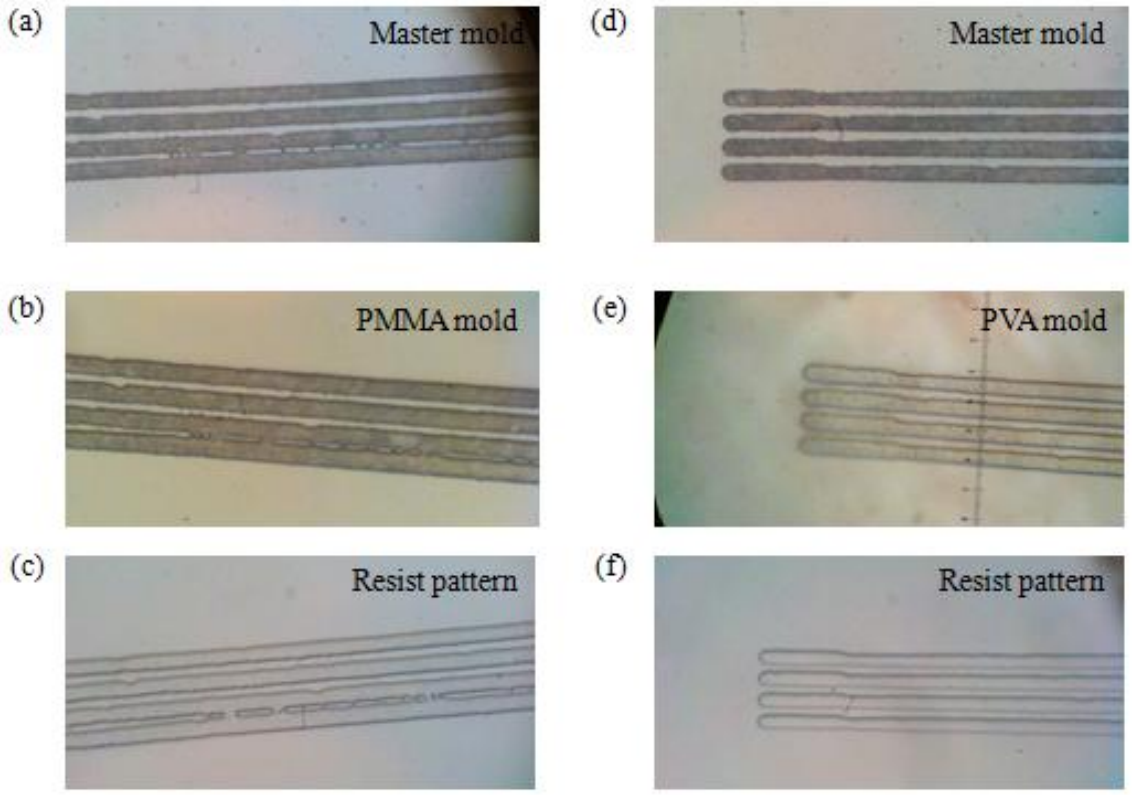

Figure 16. Comparisons between master mold, soft mold, and imprint resist pattern. (a) some features on master mold. (b) Same features as (a) on PMMA mold. (c) Imprinted features by PMMA mold. (d) other features on master mold. (e) Same features as (d) on PVA mold. (f)Imprinted features by PVA mold. Images were taken under 100X in microscope.

Features in Figure 16 are 5μm lines and the images were taken under 100X in microscope. These features are identical in size and shape in master mold, PMMA mold and imprinted

result images. Even imperfections in the master mold such as the sub-micron line spacing between the lower two lines in Figure 16(a) were successfully replicated in the bilayer resist. The results prove the capability of replicating sub-micron features using PMMA as the hard layer on the soft mold and PVA as the hard layer on the soft mold in Soft UV-NIL. However, when using H-PDMS as the hard layer in the soft mold, the imprint process was not as successful as with PMMA or PVA coated soft molds. In experiments using H-PDMS soft mold to imprint into the UV-curable M-PDMS / PMMA bilayer, the patterned M-PDMS layer could not be separated from the cured bilayer resist. This may be due to the fact that both H-PDMS and M-PDMS are functionalized PDMS compounds, perhaps leading to efficient bonding between these layers in the UV-curing step. This idea was tentatively verified by a simple test: a small amount of M-PDMS resist was dropped onto an un-patterned region of both H-PDMS and PVA molds and left in place for 10 minutes. After attempting to remove the resist layer from both surfaces, an obvious residue of the M-PDMS resist could be seen on the H-PDMS mold, while the surface of the PVA mold was found to be clear. While this result may explain the trouble encountered in the use of H-PDMS as the hard layer in the soft mold, the exact chemical interaction between these specially functionalized PDMS products needs to be investigated further. Due to these issues, the remainder of this report focuses on the imprint processes utilizing PVA or PMMA as the hard layer on the soft mold.

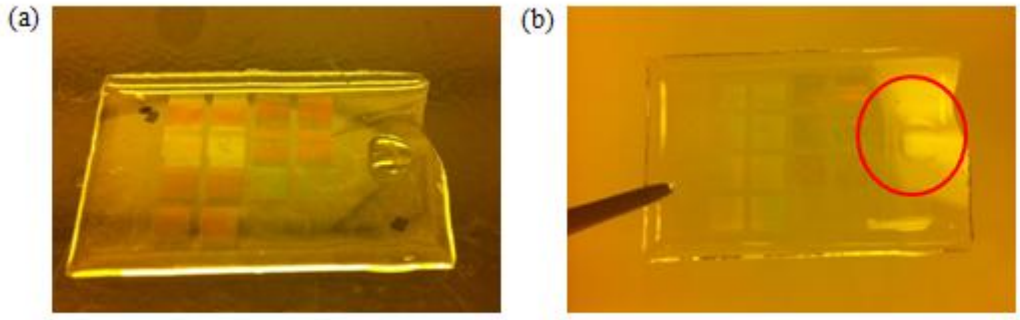

Figure 17. Test of interaction between M-PDMS and H-PDMS. (a) H-PDMS soft mold with one drop of M-PDMS resist on the side. (b) Same H-PDMS after waiting for 10 minutes and cleaned. A obvious circle pattern was left on the surface.

After separation of the soft mold from the resist substrate, RIE was performed to transfer patterns down to the substrate. As discussed in the previous chapter, undercut structures are expected to be created after pattern transfer RIE due to the different etch rates in O_2 RIE of the two resist layers used. To verify this, patterned bilayer resist samples were cleaved and investigated using a scanning electron microscope (SEM). Figure 18 presents the example SEM images of undercut structures. Because of similar secondary electron emission coefficients of these materials and possibly charging effects, the two layers of the resist are not easily distinguishable, but the presence of the anticipated undercut is clearly seen in these images.

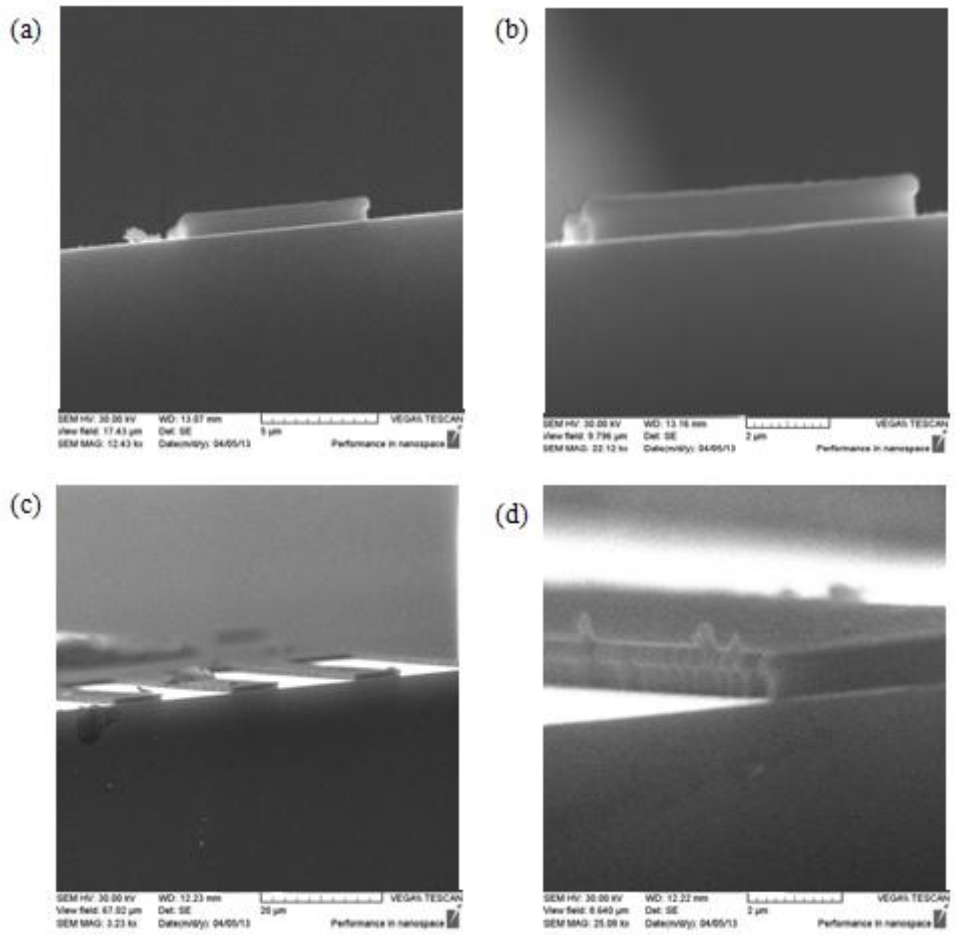

Figure 18. SEM images of undercut structures. The scale bar of each image is: (a) 5µm, (b) 2µm, (c) 20µm, and (d) 2µm.

4.1.3 Metal Deposition and Lift-off

After completion of the RIE pattern transfer, samples were covered with a thin layer of Cr by thermal metal evaporation, followed by lift-off through sonication in acetone for 2 minutes. The lift-off was successful and did not appear to leave residual PMMA on the samples. The replicated patterns are shown in Figure 19. The metal patterns show a good consistency in size and shape when comparing master mold, soft mold, and replicated metal patterns.

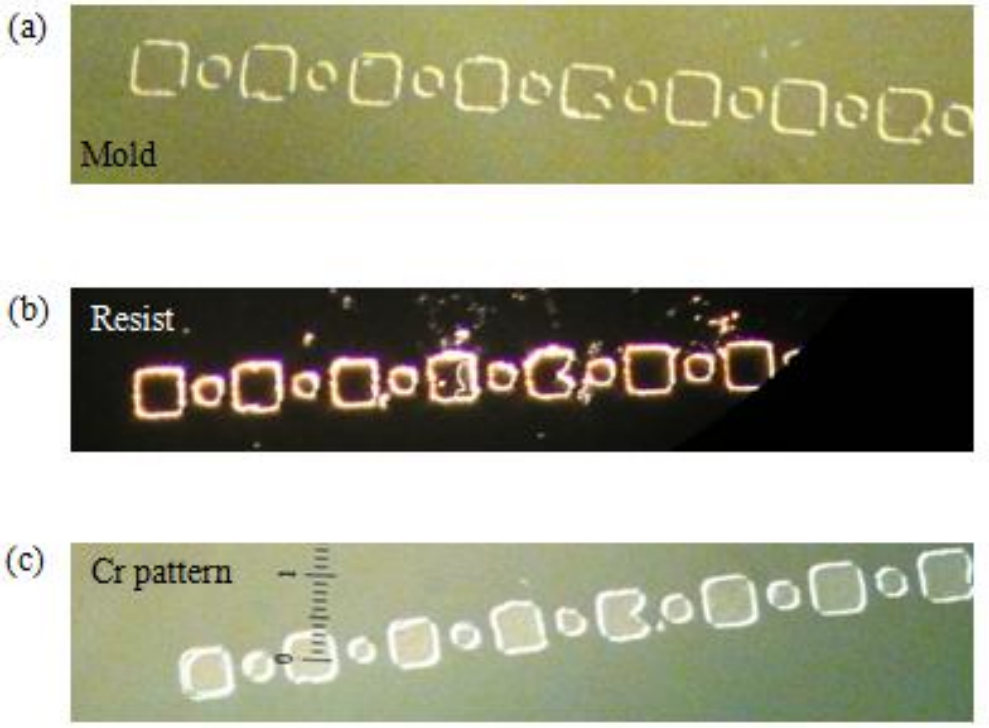

/

Figure 19. Comparison between soft mold, resist patterns, and deposited metal patterns. (a) features on soft mold, (b) features on imprinted resist, (c) deposited metal features. Images were taken under 50X in microscope.

4.2 Nanometer-scale Imprint

4.2.1 Nano Soft Mold Fabrication

For high resolution nanoimprinting a glass master mold with sub-micron feature sizes was used. The master mold was provided by Prof. Debashis Chanda (NSTC), and consisted of a glass slide coated with a spin-on-glass, with square depressions patterned into the spin-on-glass layer, as shown in Figure 19(a). Each block has its own size and periodicity. The feature sizes range from 1.1μm down to 240nm. Figures 19(b),(c),(d) show example SEM images of 1μm, 480nm, and 240nm features of the master mold. The depth of these features is approximately 400nm. The mold was treated with an anti-sticking layer of Liquid SAM prior to use.

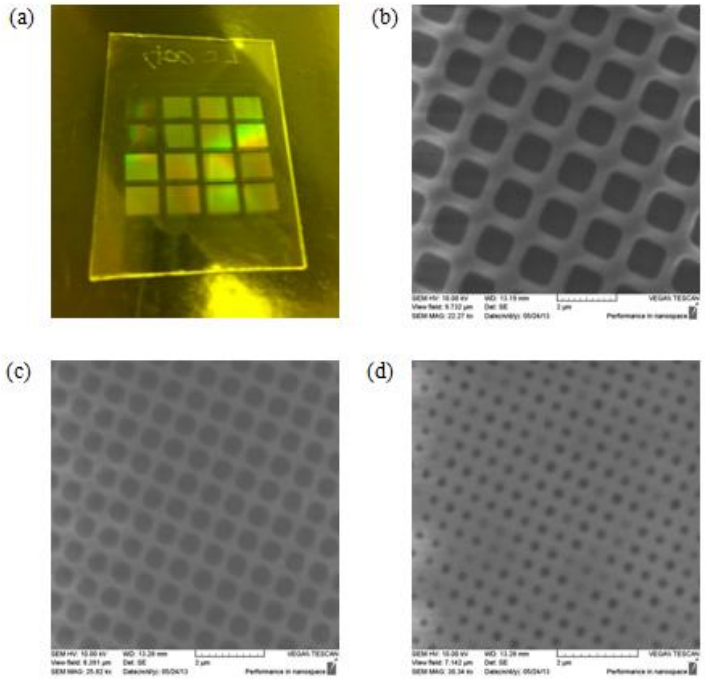

Figure 20. Demonstration of master mold for nanometer-scale imprint. (a)overview of the mold, (b)1μm features, (c)480nm features, (d)240nm features.

Soft molds were prepared using the same procedure as used for the low-resolution test patterns (Section 3.3). As in the master mold, several beautiful patterned blocks are visible due to light diffraction on the regular patterned nanostructures, see Figure 21a. This demonstrates that the periodicity of the master mold is replicated successfully over large areas. Since soft molds are insulating, they cause significant charging in SEM imaging, making it difficult to visualize the quality of the soft-mold replication step. Therefore, Atomic Force Microscopy (AFM) was attempted using a Witec Near-field Scanning Optical Microscope (AlphaSNOM) in AFM mode in order to determine the quality of the replicated soft mold and of the imprint results at the nanoscale. Figure 21(b) and (c) show a typical AFM measurement of a 550 nm feature size region on the soft mold, and a line cut through the features, respectively. Issues with sample drift or other system instability make it difficult to evaluate the pattern shape replication, however the observed pattern depth and sidewall inclination suggest good feature replication.

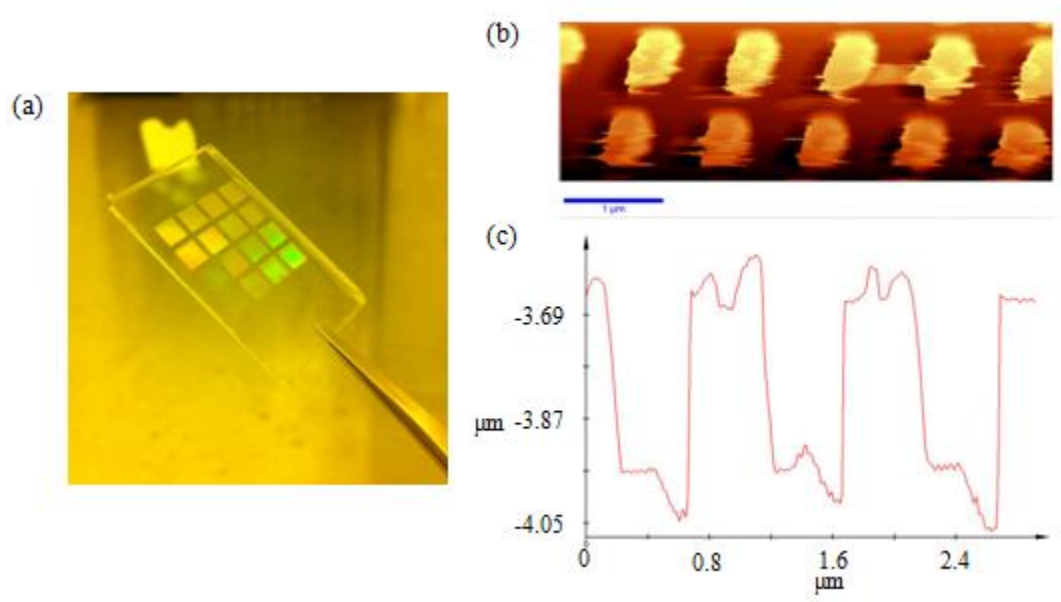

Figure 21. Demonstration of soft mold for nanometer-scale imprint. (a) overview of soft mold. AFM measurement of 280nm features (b) top view, (d) cross-section; 550nm features (c) top view, (e) cross-section.

One thing should be noted on the PVA soft mold fabrication. Since the anti-sticking coating that was already present on the provided master mold makes its surface hydrophobic, the PVA aqueous solution used to form the hard layer on the soft mold is expected to be partly blocked from filling the nanostructures on the master mold. To facilitate the PVA soft mold fabrication, the master mold was immersed in DI water overnight in order to increase the wettability of master mold's surface[45]. This effect is demonstrated in Figure 22. The master mold in both figures was covered by DI water. It's evident that, before long-term water immersion, the master mold was clearly hydrophobic, and diffraction from each pattern blocks could be clearly seen, attributed to index contrast in each feature due to incomplete

filling of the hydrophobic nanoscale depressions (Figure 21(a)). On the other hand, after long-term water immersion the surface's wettablility increased, and no clear diffracted colors from the patterned blocks are observed, attributed to improved filling of the nanoscale depressions and the index matching between the water and substrate in the patterned areas (Figure 21(b)).

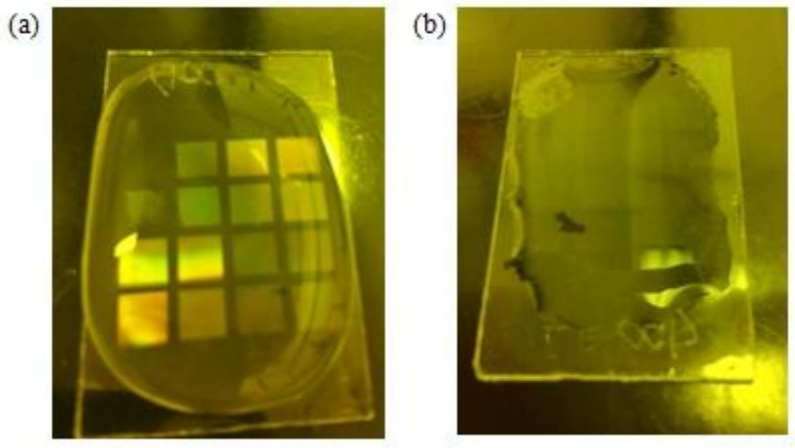

Figure 22. Example of increasing surface's wettablility by waster immersion. (a) before water immersion, (b) after water immersion.

In the course of the experiments it was found that thin-film pure PMMA and pure PVA soft molds can also be fabricated by spin-coating multiple PMMA or PVA layers on the hard master mold. The resulting soft mold could be peeled off the master mold in one piece. Figure 23 shows the resulting flexible thin-film pure PVA soft mold (right) next to the master mold (left) after three spin coating steps using the spin coating parameters listed in Table 3. . The thickness of thin-film soft mold is approximately 80 to 100μm. The resulting flexible

mold could be used for patterning non-planar samples and materials, e.g. patterning of a glass cylinder or for roll-to-roll imprint processes[35].

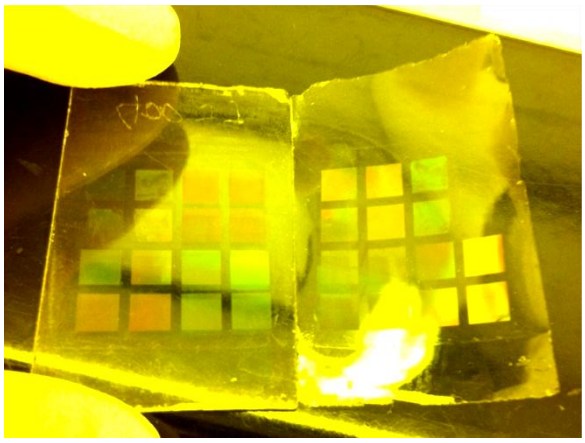

Figure 23. Demonstration of PVA thin-film mold.

4.2.2 Soft UV-NIL Results

The preparation of the bilayer resist for nanometer imprinting was similar to the process used for the low-resolution test imprint. However due to the smaller feature height of the nanostructured master mold and replicated soft mold compared to those of the low resolution soft mold, the thickness of the UV-curable resist was reduced. This is important to facilitate resist expulsion from the imprinted regions. The thickness of the bilayer resist was reduced by increasing the spin-coating speed to 7500rpm, which resulted in a resist thickness of 355nm as found using to ellipsometry. The thickness of PMMA layer was kept the same at 300nm.

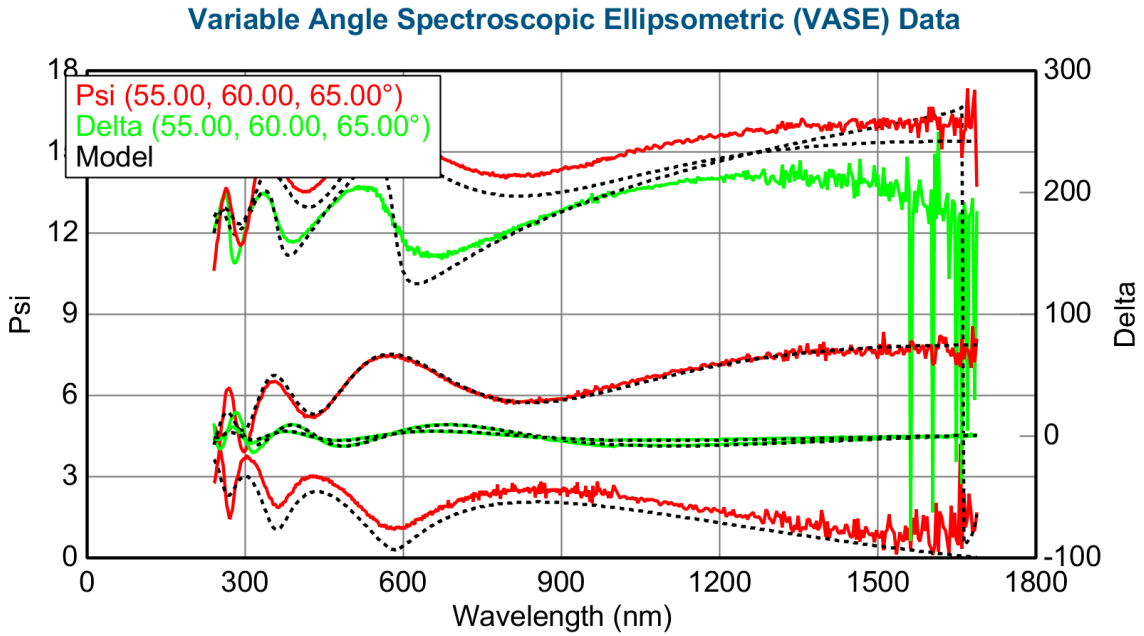

Figure 24. Ellipsometry fitting for UV resist spin-coated at 7500rpm for 90 seconds.

Table 7. Fitting parameter for M-PDMS UV resist spin coated at 7500rpm.

MSE	Roughness	Thickness	A	B	C
12.874	0.11 ± 0.527 nm	355.44± 2.794 nm	1.476 ± 0.00066674	0.00358 ± 0.00031489	9.2959E-05 ± 2.1633E-05

The UV imprinting process was done on the NX2500 using the conditions described in Section 3.5. However, for the PMMA coated nanostructured soft mold, the mold separation process after imprinting was not perfect. The PMMA layer of the soft mold was found to tear during the mold-resist separation. This is attributed to an increase in adhesion force between the mold and the resist when using a nanopatterned mold as a result of increased contact area[46] (the nanostructured soft mold has more and denser features compare to test soft mold), while the adhesion force between PMMA hard layer and PDMS buffer layer in soft mold

remains the same. Therefore, adhesion promoters for improving adhesion between the PMMA hard layer and the PDMS buffer layer are needed when using a PMMA coated soft mold for the replication of large area nanoscale features. The situation is different when using PVA as the hard layer on the soft mold. PVA has hydroxyl groups, which help in the formation of intra-molecular bonds (Si-O-C) between PVA and PDMS[47], the adhesion between PVA and PDMS is therefore expected to be larger than adhesion between resist and PVA mold. Indeed, mold-resist separation was good in each imprint attempt. Figure 25 demonstrates an overview image of an imprinted bilayer resist structure after imprinting with a PVA coated soft mold, as well as a corresponding SEM measurement. In Figures 25(b)(c)(d), the SEM images of the resist pattern show results consistent with the SEM images of the master mold shown in Figure 20(b)(c)(d).

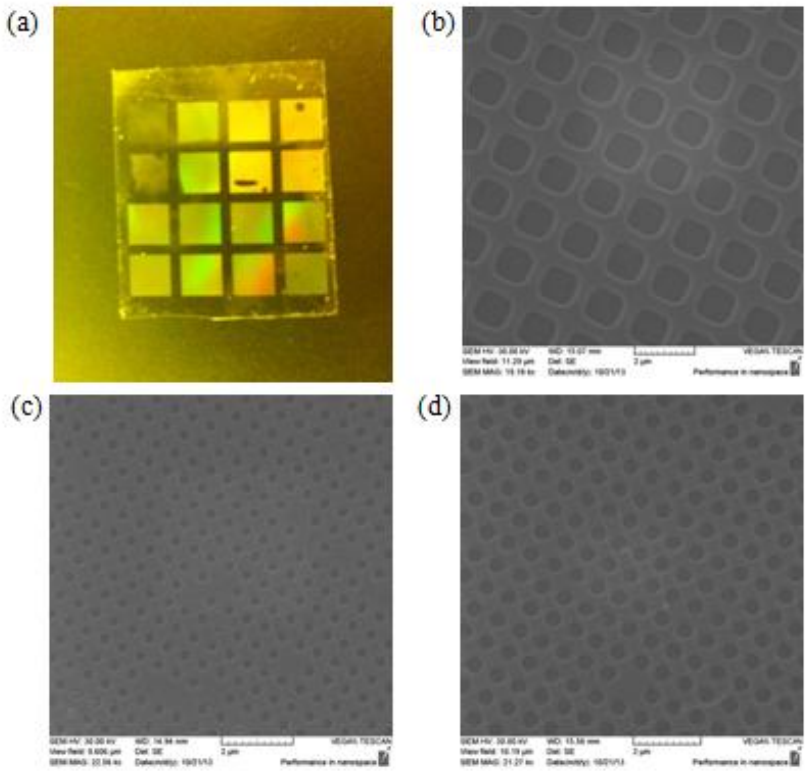

Figure 25. Nanoimprint result for PVA soft mold. (a) overall image of imprinted resist substrate. SEM images of imprinted resist pattern (b) 1µm, (c) 280nm, (d) 420nm. All scale bar are 2µm

4.2.3 Metal Deposition and Lift-off

After imprinting of the bilayer resist with the PVA coated soft mold, the sample was RIE etched to transfer patterns down to substrate, expected to result in an undercut resist edge structure. This was followed by metal deposition and lift-off. Different metals have been deposited in different imprint experiments, such as chrome, aluminum, and gold. In all cases good lift-off results were obtained. Figure 26 presents the lift-off results of Al features with (a) 1µm, (b) 420nm, and (c) and (d) 280nm features.

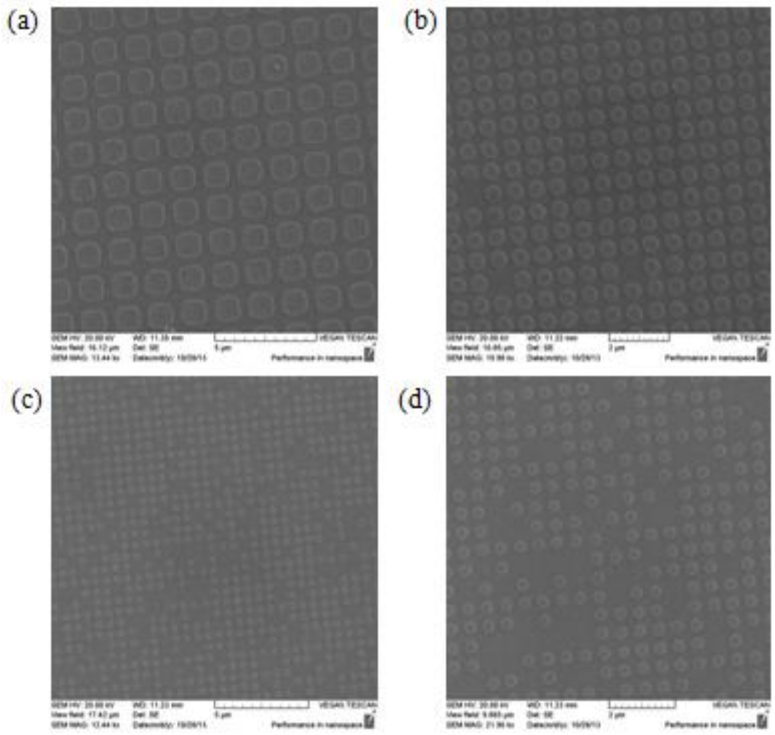

Figure 26. Lift-off results for nanometer-scale features. The scale bar is (a) 2µm, (b) 2µm, (c) 5µm, and (d) 2µm.

4.2.4 Conformal Imprinting

One advantage of using Soft mold is its conformal contact with resist. When there's a big particle either on soft mold or in UV resist, soft mold is able to slightly deform its shape to accommodate protrusions on its surface forming conformal contact with resist layer. The following figure presents the result of this advantage. In Figure 27, the black circle is the area where big particle (~10µm in size) was stuck at. Only a small area around it was affected by the big particle, deposited features still showed good uniformity on rest on the area.

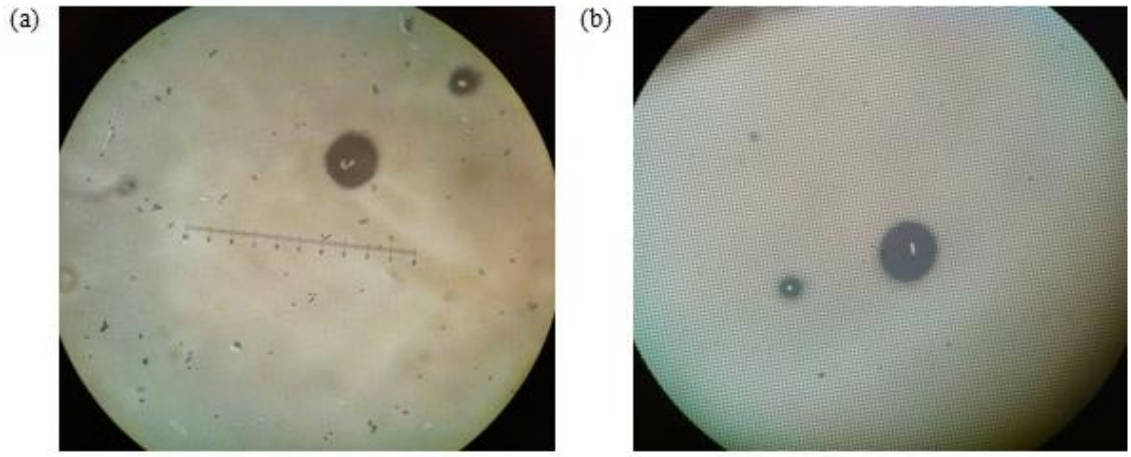

Figure 27. Big particle affected metal deposition results. Both images were 1μm features but on different samples. Images were taken under 50X in microscope.

CHAPTER FIVE: CONCLUSION

The large scale fabrication of nanostructures has become more and more important in plasmonics research. Nanoimprint Lithography (NIL) is one of the most cost-effective next-generation nanopatterning techniques. Among the various implementations of NIL, Soft UV-Nanoimprint (Soft UV-NIL) has the advantages of a simple fabrication procedure, room-temperature and low pressure processing, and low-cost mold fabrication. Therefore, a soft UV-NIL process was developed for the patterning of metallic antenna arrays in this report.

The work set the following goals: (a) the developed method should allow the replication of nanoscale patterns with minimal chance of damage to the master mold, (b) the method should allow for some degree of conformal contact to accommodate height variations in sample or mold, (c) the method should enable metal deposition and good lift-off performance. To meet these goals, the final process includes the replication of a negative hard mold to produce a positive soft-mold, followed by low-pressure imprinting of the soft mold into a low-viscosity bilayer resist where the resist layers exhibit different etch rates to enable the formation of an undercut in the replicated imprinted resist layer after pattern transfer using reactive ion etching.

Two sets of imprint experiments were carried out: micron-scale imprint experiments and nanometer-scale imprint experiments. To verify the feasibility of the complete approach micron-scale imprint runs that used a custom-designed test pattern were carried out prior to the replication of a nanometer-scale pattern.

Hard negative master molds containing the original patterns were replicated to generate positive soft molds consisting of top layer that holds the pattern, an PDMS buffer layer to allow conformal contact, backed by a glass slide. Several materials were tested as the top layer on the soft mold: Poly(methyl methacrylate) (PMMA), Hard-Polydimethylsiloxane (H-PDMS), and Polyvinyl alcohol (PVA). These materials were tested in imprint experiments on a bilayer resist consisting of a custom-mixed Methacryloxypropyl terminated Polydimethyl-siloxane (M-PDMS) based UV-curable resist film, spin-coated on a PMMA film. The resist is UV-cured in the imprint system (Nanonex NX2500) and separated from the soft mold, resulting in a negative replica of the soft mold. This pattern is processed in reactive ion etching (RIE) where the M-PDMS layer acts as an effective etching mask, resulting in exposed sections of the substrate. Metal deposition onto these areas followed by lift-off results in a positive metal replica of the features in the soft mold.

Sub-micron features were successfully replicated using both PMMA and PVA coated soft molds. Features down to 280nm were replicated successfully using PVA coated soft molds. Conformal imprinting due to the use of a soft buffer layer in the imprint mask was demonstrated.

In conclusion, a Soft UV-NIL pattern replication process was developed based on a glass-backed polymer soft mold and a custom-mixed silicon-based resist. This is a cost-effective nanofabrication technique that can be used in any research that requires replication of large-area two-dimensional patterns.

REFERENCE

1. Freestone, I.; Meeks, N.; Sax, M.; Higgitt, C., The Lycurgus Cup - A Roman nanotechnology. *Gold Bull* **2007,** *40* (4), 270-277.

2. Murray, W. A.; Barnes, W. L., Plasmonic materials. *Adv Mater* **2007,** *19* (22), 3771-3782.

3. Stockman, M. I., Nanoplasmonics: The physics behind the applications. *Phys Today* **2011,** *64* (2), 39-44.

4. Haynes, C. L.; Van Duyne, R. P., Nanosphere lithography: A versatile nanofabrication tool for studies of size-dependent nanoparticle optics. *J Phys Chem B* **2001,** *105* (24), 5599-5611.

5. Im, S. H.; Lee, Y. T.; Wiley, B.; Xia, Y. N., Large-scale synthesis of silver nanocubes: The role of HCl in promoting cube perfection and monodispersity. *Angew Chem Int Edit* **2005,** *44* (14), 2154-2157.

6. Noguez, C., Surface Plasmons on Metal Nanoparticles: The Influence of Shape and Physical Environment. *J Phys Chem C* **2007,** *111* (10), 3806-3819.

7. Anderson, L. J. E.; Payne, C. M.; Zhen, Y. R.; Nordlander, P.; Hafner, J. H., A Tunable Plasmon Resonance in Gold Nanobelts. *Nano Lett* **2011,** *11* (11), 5034-5037.

8. Gordon, T. R.; Paik, T.; Klein, D. R.; Naik, G. V.; Caglayan, H.; Boltasseva, A.; Murray, C. B., Shape-Dependent Plasmonic Response and Directed Self-Assembly in a New Semiconductor Building Block, Indium-Doped Cadmium Oxide (ICO). *Nano Lett* **2013,** *13* (6), 2857-2863.

9. Maier, S. A.; Kik, P. G.; Atwater, H. A.; Meltzer, S.; Harel, E.; Koel, B. E.; Requicha, A. A. G., Local detection of electromagnetic energy transport below the diffraction limit in metal nanoparticle plasmon waveguides. *Nat Mater* **2003,** *2* (4), 229-232.

10. Fevrier, M.; Gogol, P.; Aassime, A.; Megy, R.; Delacour, C.; Chelnokov, A.; Apuzzo, A.; Blaize, S.; Lourtioz, J. M.; Dagens, B., Giant Coupling Effect between Metal Nanoparticle Chain and Optical Waveguide. *Nano Lett* **2012,** *12* (2), 1032-1037.

11. Solis, D.; Willingham, B.; Nauert, S. L.; Slaughter, L. S.; Olson, J.; Swanglap, P.; Paul, A.; Chang, W. S.; Link, S., Electromagnetic Energy Transport in Nanoparticle Chains via Dark Plasmon Modes. *Nano Lett* **2012,** *12* (3), 1349-1353.

12. McFarland, A. D.; Van Duyne, R. P., Single silver nanoparticles as real-time optical sensors with zeptomole sensitivity. *Nano Lett* **2003,** *3* (8), 1057-1062.

13. Wu, C. H.; Khanikaev, A. B.; Adato, R.; Arju, N.; Yanik, A. A.; Altug, H.; Shvets, G., Fano-resonant asymmetric metamaterials for ultrasensitive spectroscopy and identification of molecular monolayers. *Nat Mater* **2012,** *11* (1), 69-75.

14. Sperling, R. A.; Rivera gil, P.; Zhang, F.; Zanella, M.; Parak, W. J., Biological applications of gold nanoparticles. *Chem Soc Rev* **2008,** *37* (9), 1896-1908.

15. El-Sayed, I. H.; Huang, X. H.; El-Sayed, M. A., Surface plasmon resonance scattering and absorption of anti-EGFR antibody conjugated gold nanoparticles in cancer diagnostics: Applications in oral cancer. *Nano Lett* **2005,** *5* (5), 829-834.

16. Fang, C. H.; Shao, L.; Zhao, Y. H.; Wang, J. F.; Wu, H. K., A Gold Nanocrystal/Poly(dimethylsiloxane) Composite for Plasmonic Heating on Microfluidic Chips. *Adv Mater* **2012,** *24* (1), 94-+.

17. Cho, C. Y.; Zhang, Y. J.; Cicek, E.; Rahnema, B.; Bai, Y. B.; McClintock, R.; Razeghi, M., Surface plasmon enhanced light emission from AlGaN-based ultraviolet light-emitting diodes grown on Si (111). *Appl Phys Lett* **2013,** *102* (21).

18. Chang, C. C.; Sharma, Y. D.; Kim, Y. S.; Bur, J. A.; Shenoi, R. V.; Krishna, S.; Huang, D. H.; Lin, S. Y., A Surface Plasmon Enhanced Infrared Photodetector Based on InAs Quantum Dots. *Nano Lett* **2010,** *10* (5), 1704-1709.

19. Munday, J. N.; Atwater, H. A., Large Integrated Absorption Enhancement in Plasmonic Solar Cells by Combining Metallic Gratings and Antireflection Coatings. *Nano Lett* **2011,** *11* (6), 2195-2201.

20. Wu, J.; Mangham, S. C.; Reddy, V. R.; Manasreh, M. O.; Weaver, B. D., Surface plasmon enhanced intermediate band based quantum dots solar cell. *Sol Energ Mat Sol C* **2012,** *102*, 44-49.

21. Cattoni, A.; Ghenuche, P.; Haghiri-Gosnet, A. M.; Decanini, D.; Chen, J.; Pelouard, J. L.; Collin, S., lambda(3)/1000 Plasmonic Nanocavities for Biosensing Fabricated by Soft UV Nanoimprint Lithography. *Nano Lett* **2011,** *11* (9), 3557-3563.

22. Jiang, X. M.; Ji, Q.; Ji, L. L.; Chang, A.; Leung, K. N., Resolution improvement for a maskless microion beam reduction lithography system. *J Vac Sci Technol B* **2003,** *21* (6), 2724-2727.

23. Vieu, C.; Carcenac, F.; Pepin, A.; Chen, Y.; Mejias, M.; Lebib, A.; Manin-Ferlazzo, L.; Couraud, L.; Launois, H., Electron beam lithography: resolution limits and applications. *Appl Surf Sci* **2000,** *164*, 111-117.

24. Zhang, J.; Fouad, M.; Yavuz, M.; Cui, B., Charging effect reduction in electron beam lithography with nA beam current. *Microelectron Eng* **2011,** *88* (8), 2196-2199.

25. Byun, I.; Kim, J., Cost-effective laser interference lithography using a 405 nm AlInGaN semiconductor laser. *J Micromech Microeng* **2010,** *20* (5).

26. Gan, Z. S.; Cao, Y. Y.; Evans, R. A.; Gu, M., Three-dimensional deep sub-diffraction optical beam lithography with 9 nm feature size. *Nat Commun* **2013,** *4*.

27. Tseng, A. A.; Notargiacomo, A.; Chen, T. P., Nanofabrication by scanning probe microscope lithography: A review. *J Vac Sci Technol B* **2005,** *23* (3), 877-894.

28. Smith, H. I.; Menon, R.; Patel, A.; Chao, D.; Walsh, M.; Barbastathis, G., Zone-plate-array lithography: A low-cost complement or competitor to scanning-electron-beam lithography. *Microelectron Eng* **2006,** *83* (4-9), 956-961.

29. Chou, S. Y.; Krauss, P. R.; Renstrom, P. J., Imprint of Sub-25 Nm Vias and Trenches in Polymers. *Appl Phys Lett* **1995,** *67* (21), 3114-3116.

30. Chou, S. Y.; Krauss, P. R., Imprint lithography with sub-10 nm feature size and high throughput. *Microelectron Eng* **1997,** *35* (1-4), 237-240.

31. Haisma, J.; Verheijen, M.; vandenHeuvel, K.; vandenBerg, J., Mold-assisted nanolithography: A process for reliable pattern replication. *J Vac Sci Technol B* **1996,** *14* (6), 4124-4128.

32. Belotti, M.; Torres, J.; Roy, E.; Pepin, A.; Gerace, D.; Andreani, L. C.; Galli, M.; Chen, Y., Fabrication of SOI photonic crystal slabs by soft UV-nanoimprint lithography. *Microelectron Eng* **2006,** *83* (4-9), 1773-1777.

33. Barbillon, G.; Hamouda, F.; Held, S.; Gogol, P.; Bartenlian, B., Gold nanoparticles by soft UV nanoimprint lithography coupled to a lift-off process for plasmonic sensing of antibodies. *Microelectron Eng* **2010,** *87* (5-8), 1001-1004.

34. Jung, H. Y.; Hwang, S. Y.; Bae, B. J.; Lee, H., Lift-off process using bilayer ultraviolet nanoimprint lithography and methacryloxypropyl-terminated-polydimethylsiloxane-based imprint resin. *J Vac Sci Technol B* **2009,** *27* (4), 1861-1864.

35. Hwang, S. Y.; Hong, S. H.; Jung, H. Y.; Lee, H., Fabrication of roll imprint stamp for continuous UV roll imprinting process. *Microelectron Eng* **2009,** *86* (4-6), 642-645.

36. Wang, J. J.; Chen, L.; Liu, X. M.; Sciortino, P.; Liu, F.; Walters, F.; Deng, X. G., 30-nm-wide aluminum nanowire grid for ultrahigh contrast and transmittance polarizers made by UV-nanoimprint lithography. *Appl Phys Lett* **2006,** *89* (14).

37. Faircloth, B.; Rohrs, H.; Tiberio, R.; Ruoff, R.; Krchnavek, R. R., Bilayer, nanoimprint lithography. *J Vac Sci Technol B* **2000,** *18* (4), 1866-1873.

38. Jung, G. Y.; Wu, W.; Ganapathiappan, S.; Ohlberg, D. A. A.; Islam, M. S.; Li, X.; Olynick, D. L.; Lee, H.; Chen, Y.; Wang, S. Y.; Tong, W. M.; Williams, R. S., Issues on nanoimprint lithography with a single-layer resist structure. *Appl Phys a-Mater* **2005,** *81* (7), 1331-1335.

39. Odom, T. W.; Love, J. C.; Wolfe, D. B.; Paul, K. E.; Whitesides, G. M., Improved pattern transfer in soft lithography using composite stamps. *Langmuir* **2002,** *18* (13), 5314-5320.

40. Shi, J.; Peroz, C.; Peyrade, D.; Salari, J.; Belotti, M.; Huang, W. H.; Chen, Y., Tri-layer soft UV imprint lithography and fabrication of high density pillars. *Microelectron Eng* **2006,** *83* (4-9), 1664-1668.

41. Cattoni, A.; Cambril, E.; Decanini, D.; Faini, G.; Haghiri-Gosnet, A. M., Soft UV-NIL at 20 nm scale using flexible bi-layer stamp casted on HSQ master mold. *Microelectron Eng* **2010,** *87* (5-8), 1015-1018.

42. Schmid, H.; Michel, B., Siloxane polymers for high-resolution, high-accuracy soft lithography. *Macromolecules* **2000,** *33* (8), 3042-3049.

43. Kim, H. D.; Nakayama, T.; Yoshimura, J.; Imaki, K.; Yoshimura, T.; Suematsu, H.; Suzuki, T.; Niihara, K., Fabrication of the finestructured alumina materials with nanoimprint method. *J Ceram Soc Jpn* **2009,** *117* (1364), 534-536.

44. Korea, M. T., http://www.minuta.co.kr/products/products_new2.html.

45. Ma, K.; Rivera, J.; Hirasaki, G. J.; Biswal, S. L., Wettability control and patterning of PDMS using UV-ozone and water immersion. *J Colloid Interf Sci* **2011,** *363* (1), 371-378.

46. Jung, G. Y.; Li, Z. Y.; Wu, W.; Ganapathiappan, S.; Li, X. M.; Olynick, D. L.; Wang, S. Y.; Tong, W. M.; Williams, R. S., Improved pattern transfer in nanoimprint lithography at 30 nm half-pitch by substrate-surface functionalization. *Langmuir* **2005,** *21* (14), 6127-6130.

47. Emoto, A. K., T; Noguchi, N; Fukuda, T, Tailoring Adhesive Forces Between Poly(dimethylsiloxane) and Glass Substrates Using Poly(vinyl alcohol) Primers. *J Appl Polym Sci* **2013**.